STEM CELLS AND DEVELOPMENT
Volume 22, Number 10, 2013

DOI: 10.1089/scd.2012.0150

Dopamine Receptors in Human Embryonic Stem Cell Neurodifferentiation

Glenn S. Belinsky, Carissa L. Sirois, Matthew T. Rich, Shaina M. Short, Anna R. Moore, Sarah E. Gilbert, and Srdjan D. Antic

We tested whether dopaminergic drugs can improve the protocol for in vitro differentiation of H9 human embryonic stem cells (hESCs) into dopaminergic neurons. The expression of 5 dopamine (DA) receptor subtypes (mRNA and protein) was analyzed at each protocol stage (1, undifferentiated hESCs; 2, embryoid bodies [EBs]; 3, neuroepithelial rosettes; 4, expanding neuroepithelium; and 5, differentiating neurons) and compared to human fetal brain (gestational week 17–19). D2-like DA receptors (D2, D3, and D4) predominate over the D1-like receptors (D1 and D5) during derivation of neurons from hESCs. D1 was the receptor subtype with the lowest representation in each protocol stage (Stages 1–5). D1/D5-agonist SKF38393 and D2/D3/D4-agonist quinpirole (either alone or combined) evoked Ca^{2+} responses, indicating functional receptors in hESCs. To identify when receptor activation causes a striking effect on hESC neurodifferentiation, and what ligands and endpoints are most interesting, we varied the timing, duration, and drug in the culture media. Dopaminergic agonists or antagonists were administered either early (Stages 1–3) or late (Stages 4–5). Early DA exposure resulted in more neuroepithelial colonies, more neuronal clusters, and more TH^+ clusters. The D1/D5 antagonist SKF83566 had a strong effect on EB morphology and the expression of midbrain markers. Late exposure to DA resulted in a modest increase in TH^+ neuron clusters ($\sim$75%). The increase caused by DA did not occur in the presence of dibutyryl cAMP (dbcAMP), suggesting that DA acts through the cAMP pathway. However, a D2-antagonist (L741) decreased TH^+ cluster counts. Electrophysiological parameters of the postmitotic neurons were not significantly affected by late DA treatment (Stages 4–5). The mRNA of mature neurons (*VGLUT1* and *GAD1*) and the midbrain markers (*GIRK2*, *LMX1A*, and *MSX1*) were lower in hESCs treated by DA or a D2-antagonist. When hESCs were neurodifferentiated on PA6 stromal cells, DA also increased expression of tyrosine hydroxylase. Although these results are consistent with DA's role in potentiating DA neurodifferentiation, dopaminergic treatments are generally less efficient than dbcAMP alone.

Introduction

The actions of catecholamine neurotransmitter dopamine (DA) produced by neurons in the midbrain, hypothalamus, and olfactory bulb have been the subject of intense interest due to its roles in neurological disorders [1–3]. Tyrosine hydroxylase (TH) expression, a hallmark of dopaminergic and noradrenergic neurons, is found in the human fetal brain before all cortical layers have been formed [4–6], suggesting that at this early age DA is involved in proliferation, migration, and differentiation of young neurons [7–9]. Ambient DA was detected in follicular fluid of superovulated women [10], and human fetal brain tissue (9–10 gestational weeks [GWs]) in vitro [11]. All together, these findings imply that human neurodifferentiation may be regulated by DA.

There is an ongoing effort to optimize stem cell differentiation protocols for use in cell replacement therapy of Parkinson's disease [12–14]. Large numbers of transplanted neurons are necessary for their survival and integration into the host brain [15,16]. The number of surviving neurons in the host brain is considered the primary determinant of the efficacy of any cell replacement therapy, including the therapy of Parkinson's disease [17]. In vitro production of a large number of healthy human DA neurons is therefore, a desirable goal [13,18–20].

One of the simplest differentiation protocols for deriving dopaminergic neurons from human embryonic stem cells (hESCs) uses dibutyryl cAMP (dbcAMP) during the final differentiation stage [20–22]. Drugs, such as forskolin and isobutylmethylxanthine that activate the cAMP signaling pathway (similar to dbcAMP) have also been used successfully in dopaminergic differentiation protocols [23,24]. This raises the question of whether the natural ligand DA can replace or outperform artificial cAMP stimulators (eg,

Department of Neuroscience, University of Connecticut Health Center, Farmington, Connecticut.

dbcAMP or forskolin) in dopaminergic differentiation protocols. Dopaminergic signaling is not entirely based on the cAMP pathway. DA binds to multiple receptors that can stimulate several G proteins [25,26] and thus, activate intracellular pathways different from those activated by dbcAMP alone [22,27]. The current study investigates whether DA treatment can improve the yield and quality of hESC-derived DA neurons.

Materials and Methods

Human fetal tissue

Human fetal brain tissue samples originated from the Brain Bank, Albert Einstein College of Medicine, Bronx, New York, with the postmortem delay of ~5 h. Handling of the human material was done with special care following all necessary requirements and regulations set by the institutional ethics committees. In the first specimen (GW 19), the cortical slices were microdissected into 2 halves. The pial half was termed "cortical plate" (Fig. $1B_1$; CP); the ventricular half was termed "subventricular zone" (Fig. $1B_1$; SVZ). In the second specimen (GW 17), microdissection was not performed; hence, all cortical zones were homogenized together, and termed "cortex" (Fig. $1B_1$; Cx). Both medial and lateral ganglionic eminences were included in the sample marked "GE" in Fig. $1B_1$. Total human brain RNA from an 18-year-old man was purchased from Clontech (Mountain View, CA) (Fig. $1B_1$; human adult brain).

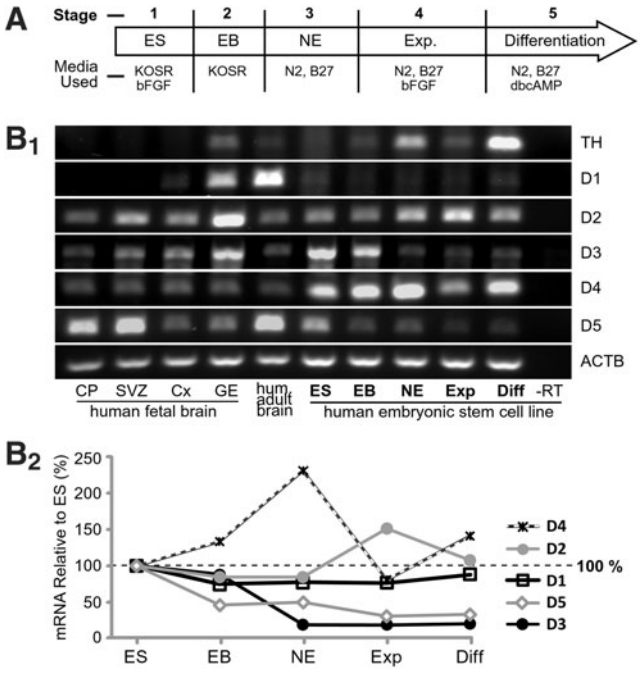

FIG. 1. Dopamine (DA) receptor mRNA levels during the dibutyryl cAMP (dbcAMP)-based differentiation protocol. **(A)** Time course of the differentiation protocol indicating media additives during each stage (Stages 1–5). **(B_1)** rtPCR of tyrosine hydroxylase (TH), 5 DA receptors, and the housekeeping gene *ACTB*. CP, cortical plate; SVZ, subventricular zone; Cx, cortex with all zones included; GE, ganglionic eminence; ES, stage 1 undifferentiated H9 human embryonic stem cell (hESC) colonies; EB, stage 2 embryoid bodies; NE, stage 3 neuroepithelia; Exp, stage 4 expansion of neuroepithelia; Diff., stage 5 final neurodifferentiation. **(B_2)** Quantitation of hESC band intensities relative to Stage 1 (ES). rtPCR, reverse transcriptase PCR.

hESC culture

All cell culture reagents were from Invitrogen (Grand Island, NY) unless otherwise noted. H9 cells ("WA09," NIH reg. No. 0062), p 50–65, were obtained from the UConn Stem Cell Core. H9 cells were cocultured with mouse embryonic fibroblasts (MEFs) in hESC media consisting of 80% DMEM/F12, 20% KOSR, 1 mM glutamine, 1× NEAA, 4 ng/mL bFGF, and 7 nL/mL β-mercapto ethanol (βME) (Sigma, St. Louis, MO). Cells were grown on plastic dishes (Nunc, Rochester, NY) coated with 0.1% porcine gelatin (Sigma). Media were changed daily and cells split using 1 mg/mL collagenase. SKF38393, quinpirole, and DA were purchased from Sigma, while SKF83566 and L741,626 from Tocris (Minneapolis, MN).

Neuronal differentiation of hESCs

H9 cells were differentiated using a dbcAMP protocol [21,22]. The differentiation process consisted of 5 stages, starting with undifferentiated hESCs (Fig. 1A; Stage 1). H9 colonies were dissociated by collagenase, and stem cell aggregates incubated for 3–4 days in hESC media without bFGF, on Ultralow adherence plates (Costar, Wilkes Barre, PA) (Stage 2). hESC aggregates were then seeded on dishes coated with 1:100 Geltrex, and allowed to expand for 4–8 days in NEP-basal medium (Stage 3) until neuroepithelial colonies appeared. NEP-basal medium consisted of DMEM/F12, 1 mg/mL BSA, 1× N2, 1× B27 supplements, and 1× penicillin/streptomycin/antimycotic. Colonies with neuroepithelial morphology were removed by trituration, and seeded on plates coated with 1:100 Geltrex. Cells were then grown in NEP-basal medium with 20 ng/mL bFGF for 7 days (Expansion, Stage 4). Cells were then maintained in NEP-basal medium with 1 mM dbcAMP (Sigma) for 7 days, unless otherwise noted, with the treatments indicated in the figures (Differentiation, Stage 5). For intermittent treatment, DA (Sigma) was added for 3–4 h each day during the expansion and differentiation stages using concentrations indicated in the figures. As an alternative differentiation protocol, PA6 mouse stromal cells (Riken, Japan) were used in coculture with hESCs. PA6 cells were grown in 90% MEMalpha, 10% FBS, supplemented with 1× penicillin/streptomycin/antimycotic and 2 mM glutamine. PA6 cells were seeded on glass coverslips in 24-well plates, 4×10^4 cells per well. The following day, colonies of hESC H9 cells from one 35-mm-diameter well were seeded on the PA6 feeder layers, in 90% GMEM, 10% KOSR, 1 mM Na-pyruvate, 1× nonessential amino acids, 2 mM glutamine, and 7 nL/mL βME. Media were changed daily with the subsequent addition of 1, 10, and 100 μM DA. After 14 days, cells were fixed and immunofluorescent staining performed.

mRNA expression

H9 cells at each stage of differentiation were lysed in Trizol (Invitrogen), and RNA purified according to the manufacturer's instructions. To remove any genomic DNA, all RNA was treated with DNase (NEB, Ipswich, MA). RNA integrity was verified by the presence of prominent 28s and

18s bands on ethidium-stained gels. cDNA was made from 500 ng of each sample using SuperscriptIII reverse transcriptase (Invitrogen) according to the manufacturer's instructions with both 0.94 μM oligo(dT))$_{20}$ and 4 μM random hexamers in the reaction. The following primers were used to perform polymerase chain reaction (PCR):

D1 ***F*** 5′CAGTCCACGCCAAGAATTGCC, ***R*** 5′ATTGC ACTCCTTGGAGATGGAGCC;
D2 ***F*** 5′GCAGACCACCACCAACTACC, ***R*** 5′GGAGC TGTAGCGCGTATTGT;
D3 ***F*** 5′TGGCTGCAGGAGCCGAAGT, ***R*** 5′GAGGGCA GGACACAGCAAAGGC;
D4 ***F*** 5′CCCACCCCAGACTCCACC, ***R*** 5′GAACTCGGCG TTGAAGACAG;
D5 ***F*** 5′GTCGCCGAGGTGGCCGGTTAC, ***R*** 5′GCTGG AGTCACAGTTCTCTGCAT;
TH ***F*** 5′GGTTCCCAAGAAAAGTGTCAG, ***R*** 5′GGTGTAG ACCTCCTTCCAG;
PAX6 ***F*** 5′AGCCCAGTATAAGCGGGAGTGC, ***R*** 5′TCC CCCTCCTTCCTGTTGCTGG
PPIA ***F*** 5′CCAGGCTCGTGCCGTTTTGC, ***R*** 5′GATGG ACTTGCCACCAGTGCCA;
HPRT ***F*** 5′GACTTTGCTTTCCTTGGTCA, ***R*** 5′GGCTTT GTATTTTGCTTTTCC;
βACT ***F*** 5′CCTCGCCTTTGCCGATCC, ***R*** 5′GATGC CGTGCTCGATGGGGT.

The following primers and probes were used for quantitative PCR:

ACTB ***F*** 5′CCTCGCCTTTGCCGATCC, ***R*** 5′GCGAAGC CGGCCTTGCACAT
Probe: 5′famATGATATCGCCGCGCTCGTCGTCGAbhq
GAD1 ***F*** 5′CGACACCGGGGACAAGGCAATT, ***R*** 5′CCG TCGTTGAGGGCTGTCTGG
Probe: 5′fam CAATGGCGAGCCTGAGCACACAAACG TCTGbhq
GIRK2 ***F*** 5′CTGGAAATTGTGGTCATC, ***R*** 5′GGTCTCA TAGGTCTCATG
Probe: 5′fam AGCCACAGGGATGACATGCCbhq
LMX1A ***F*** 5′ATGCCTGGAGACCACATG, ***R*** 5′TGGAG TACAGATGGTCAATGG
Probe: 5′fam ACCCTTATGGTGCCGAGCCCbhq
MSX1 ***F*** 5′CGCTCGTCAAAGCCGAGAGCC, ***R*** 5′CGCG GCTTACGGTTCGTCTTGT
Probe: 5′fam AGAGGACCCCGTGGATGCAGAGCCCC bhq
PAX6 ***F*** 5′TCTTTGCTTGGGAAATCCG, ***R*** 5′CTGCCC GTTCAACATCCTTAG
Probe: 5′fam TCATACATGCCGTCTGCGCCCATCTGbhq
TUBB3 ***F*** 5′GGGAGGAACCCCAGGCAGCTAGA, ***R*** 5′AAGTCCGAGTCGCCCACGTAGT
Probe: 5′fam ACGTGCCTCGAGCCATTCTGGTGGbhq
VGLUT1 ***F*** 5′CAGGAGGATTTATCTGTCAAAAAT, ***R*** 5′GGGTATGTGACCCCCTCTACCAAC
Probe: 5′fam ATGCTGATCCCCTCAGCTGCCCGCbhq

PCR was performed with GoTaq polymerase (Promega, Madison, WI) using the following conditions: 94°C-4 min, [94°C-30 s, 55°C-30 s, 72°C-30 s, 72°C-10 min], for 31 cycles, except for *PPIA*, *HPRT*, and *βACT* which were performed for 27 cycles for the reactions to be in the exponential phase. PCR products were visualized on ethidium-stained gels. Band intensities were quantified with ImageJ (NIH). All bands were normalized to *ACTB*, and then divided by expression in the ES. qPCR was performed using BHQ-FAM labeled probes (Sigma) with the amplicon designed to span a splice junction wherever possible. Samples were run on an Eppendorf Realplex^2 (Hauppauge, NY) for 94°C-3 min, [94°C-30 s, 48°C–60°C-30 s, 72°C-30 s] 45 cycles, with annealing temperature dependant on the primers, using GoTaq polymerase. The delta-delta Ct method was used to quantitate results. All treatments were normalized to control and corrected for loading using the *ACTB* housekeeping gene.

Western blots

Cells or tissue were lysed in RIPA buffer (Sigma) containing 1 mM PMSF, 2.1 mM AEBSF, 1.6 μM Aprotinin, 80 μM Bestatin, 28 μM E-64, 40 μM Leupeptin, 30 μM Pepstatin A, 2 mM sodium orthovanadate, and 25 mM sodium fluoride. Protein assays were performed by BCA assay (Pierce, Rockford, IL) using BSA as a standard. Before loading, extracts were brought to 2% SDS, 5% βME, 10% glycerol, 0.01% bromophenol blue, and heated to 95°C for 5 min. ColorPlus prestained proteins (NEB) were used as molecular weight markers. 15 or 12 lane gradient mini gels (BioRad, Hercules, CA) were loaded with 20–33 μg per lane then transferred to PVDF membrane (BioRad) according to the manufacturer's instructions. The following antibodies were used, rabbit anti-D1 (1:300 Chemicon AB1784P, Billerica, MA), rat anti-D1 (1:200 Sigma d187), rabbit anti-D2 (1:300 Chemicon AB5084P), rabbit anti-D5 (1:300 Chemicon AB9509), rabbit anti-TH (1:500 Pel-Freez P40101, Rogers, AR), rabbit anti-GAPDH (1:200 Santa Cruz Biotech. sc25778, Santa Cruz, CA), anti-rabbit IgG-HRP (1:2000 Santa Cruz sc-2301), and anti-rat IgG-HRP (1:2000 Santa Cruz sc-2006). Membranes were blocked for 1–3 h with 5% nonfat dry milk in PBS. Primary antibody incubations were carried out overnight in PBS, 0.05% tween-20, and 0.5% BSA at 4°C. Membranes were washed 4 × 5 min with PBS + 0.05% tween-20, then secondary antibody incubation done in PBS, 0.05% tween-20, and 0.1% BSA for 1.5 h. After 4 × 5 min washes with PBS, bands were visualized using ECL chemiluminescent reagent (GE Healthcare, Pittsburgh, PA), and images captured on a GBox imager (Syngene, Frederick, MD).

Immunofluorescence

After differentiation, cells were fixed 30 min in 4% paraformaldehyde. Immunofluorescence was performed using 1:500 rabbit anti-TH (Pel-Freez) and 1:1000 mouse Anti-β-Tubulin III (TUJ1; Sigma T5076) antibodies. Cells were permeabilized in 0.2% Triton TM × 100 (Acros, Geel, Belgium). Cells were washed in PBS then blocked for 1 h in 10% normal goat serum, 0.75% BSA in PBS, then incubated overnight at 4°C with primary antibodies diluted in blocking solution. Cells were washed in PBS then secondary antibodies incubated for 1 h at room temperature. Goat anti-mouse Alexafluor488 and goat anti-rabbit Alexafluor594 were used in 10% goat serum. Cells were washed in PBS then incubated 10 min in 1 μg/mL Hoechst 333258 (Sigma). Cells were mounted with FluoromountG (Southern Biotech, Birmingham, AL). 2.5× images were captured by selecting colonies in the TUJ1

channel. TH and TUJ1 signals were quantified by integrating total optical density for the entire image after subtracting background using ImageJ software. Total TUJ1 fluorescence on entire coverslips was captured with 2-min exposures using a Kodak 2000MM Imager (Woodbridge, CT) with excitation 465WA and emission 535WA filters. Signal and area were quantified using ImageJ software after background subtraction. A tangled mass of $TUJ1^+$ neurons sometimes contained 2 or more clusters of putative DA cells (TH^+). Clusters containing 10 or more TH^+ cells were counted for comparison between DA-treated colonies (DA) and untreated colonies grown in regular media (Control). This allowed us to use the entire population on the surface of a coverslip for quantification.

Electrophysiology

Whole cell patch clamp recordings were performed as previously described [28]. Briefly, cells grown on 12-mm round coverslips were transferred to an Olympus BX51WI upright microscope (equipped with infrared video microscopy) and perfused in aerated (95% O_2/5% CO_2) artificial cerebrospinal fluid (ACSF) at 30°C. The ACSF contained 125 mM sodium chloride, 2.3 mM potassium chloride, 23 mM sodium bicarbonate, 1 mM magnesium sulfate, 1.26 mM monopotassium phosphate, 2 mM calcium chloride, and 10 mM glucose (pH 7.3). Individual cells were selected for recordings based on a small round or ovoid cell body (diameters 5–15 μm) and typically two or more extended processes. Pipettes (10 MΩ) were filled with an intracellular solution containing (in mM): 135 K-glutamate, 10 HEPES, 2 magnesium chloride, 3 ATP-Na_2, 0.3 GTPNa_2, and 10 P-creatine Na_2 (pH 7.3). Recordings were performed using Multiclamp 700B and Clampex 9.2 (Molecular Devices, Union City, CA). In voltage clamp configuration, cells were given a series of 10 mV voltage steps (duration, 50 ms) from −90 to +30 mV from a holding potential of −70 mV. In current clamp configuration we measured the resting membrane potential, and then a negative holding direct current (in the range: −2 to −15 pA) was applied to bring the membrane potential to approximately −60 mV. This was done to compare neurons under identical conditions during action potential (AP) firing. To assess the AP firing pattern, in current clamp configuration, we applied a series of 10 pA current steps from −20 to +60 pA. Current intensities were modified depending on cell input resistance. Electrical traces were analyzed using Clampfit 9.2 (Molecular Devices). Peak sodium current was defined as maximal transient inward current at any command voltage. Peak potassium current was measured at 40 ms from the onset of the "+30 mV" command voltage pulse.

Intracellular Ca^{2+} response

hESC colonies were loaded with Oregon green 488 Bapta-1 AM (OGB-1 AM) purchased from Invitrogen (Cat. No. 06807). To prepare the OGB-1 stock, the content of one original vial (50 μg) was dissolved in 2 μL of 20% Pluronic F-127 and 8 μL of DMSO, vortexed for 30 min, then 90 μL DMEM/F12 was added. To load hESCs, 3.33 μL of stock was added to a well containing one glass coverslip and 0.5 mL of DMEM/F12 media, incubated for 30 min and washed with warm DMEM/F12 media. After 45 min of incubation, glass coverslips were transferred to a recording chamber positioned under Olympus BX51WI and perfused with aerated saline (standard 2 mM Ca^{2+} ACSF) or "near zero calcium" ACSF (0.1 mM Ca^{2+}). hESC colonies were illuminated with computer-controlled LED (460 nm; Luminus Devices, Inc., Billerica, MA) and imaged using the RedShirtImaging System described by Zhou and Antic [29]. To improve signal-to-noise ratio, pixel outputs were spatially averaged (9–16 pixels per region of interest [ROI]) and filtered Gaussian low-pass cutoff 0.4 Hz. Signal amplitudes are reported as $\Delta F/F$ (%). Focal application of drugs was achieved using microiontophoresis as described by Zhou and Antic [29]. Concentration of drugs inside the iontophoretic pipette [in mM]: ATP [100], SKF38393 [40], quinpirole (QP) [40], and SKF + QP [40 each]. The numbers of failed attempts to trigger Ca^{2+} release are reported in the "Results" section for each experimental drug. Zero responses were eliminated from the reports of mean signal amplitude and statistical comparisons.

Statistics

Statistical analysis was performed using SigmaStat 2.03 (Systat, San Jose, CA). If data were normally distributed and variances equal, then we used Student's *t*-test, or ANOVA followed by a Tukey test for pairwise comparisons. If data points did not pass these criteria, then we used a Mann–Whitney test or Kruskal–Wallis one-way analysis of variance on ranks followed by Dunn's method for pairwise comparisons or a chi-squared test.

Results

hESCs (line H9) were differentiated using the dbcAMP-based DA differentiation protocol [22] divided into 5 stages (Fig. 1A). In our hands, this protocol regularly produces physiologically competent dopaminergic neurons [21].

mRNA in hESCs undergoing differentiation

At each stage of the differentiation protocol (Fig. 1A; Stages 1–5) mRNA levels for TH and DA receptors were examined along with human fetal brain tissue in the 17th or 19th week of gestation (Fig. $1B_1$). At this gestational age (2nd trimester) there is massive proliferation of neurons in the developing human cerebral cortex [30]. The highest TH mRNA expression was detected in the final differentiation stage of our protocol (Fig. $1B_1$; Diff.); thus, suggesting the presence of dopaminergic neurons 2 weeks after the re-seeding of neuroepithelial rosettes (Stage 5). Band intensities were first normalized to the housekeeping gene *ACTB* and then displayed relative to the expression in hESCs (Fig. $1B_1$; ES band). We found relatively low expression of mRNAs for the cAMP-stimulative D1 and D5 receptors throughout the dbcAMP-based differentiation protocol, beginning with hESCs and ending with cells in the final differentiation stage (Fig. $1B_2$; line plots D1 and D5). hESC D1 receptor bands were visible by reverse transcriptase PCR (rtPCR) only in overexposed images (Fig. $1B_1$; D1). D5 receptor mRNA was highest in undifferentiated hESCs, and its levels declined through Stages 2–5 (Fig. $1B_2$; line plot D5). Interestingly, strong bands of D5 message appeared in the human fetal cerebral cortex at 19th GW (Fig. $1B_1$; CP and SVZ). The no reverse transcriptase control yielded no bands (Fig. $1B_1$; -RT).

RNA material from MEFs cultures yielded no bands for all genes tested except for *ACTB* gene, where a faint band was present (data not shown).

In contrast to D1 and D5, the cAMP-inhibitory DA receptors D2 and D3 occasionally showed similar expression levels in our cultures as in the human fetal brain (Fig. $1B_1$, B_2). The temporal profiles of D2 and D3 receptor mRNA were opposite to each other. While D2 appeared to increase, D3 mRNA expression appeared to decline with the course of hESC neurodifferentiation (Fig. $1B_2$; line plots D2 and D3). D2 receptor mRNA showed the highest expression in Stage 4, when reseeded neuroepithelial cells were dividing and migrating (expanding) in culture. The relative expression of D3 was highest in undifferentiated ESCs (Fig. $1B_2$; ES). D3 receptor mRNA expression was reduced at the very first neurodifferentiation step (embryoid body [EB]), and it continued to decline as the differentiation protocol progressed through Stages 3, 4, and 5 (Fig. $1B_2$). The cAMP-inhibitory receptor D4 had the overall strongest expression among all D2-like receptors (D2, D3, and D4), reaching its peak in Stage 3, when neuroepithelial rosettes (NE) dominate our cultures. In fact, D4 mRNA gave the strongest signal compared to all 5 DA receptor subtypes. The D4 expression was ~2 times higher, while D2 expression was ~2-fold lower in hESC cultures than in the fetal GE. Finally, at GW 17, the GE (precursor of the neostriatal medium spiny neurons) is rich in both D1-like and D2-like DA receptor families, consistent with D1 and D2 expression in adult basal ganglia [31]. At GW 19, however, D5 was the dominant DA receptor in the developing cerebral cortex (Fig. $1B_1$; CP and SVZ), followed by the D2 receptor subtype.

Proteins in differentiating hESCs

The same 5 stages of hESC neurodifferentiation and the same human fetal brain tissue samples described in Fig. 1 were next used to study DA receptor protein levels (by western blot). In the hESC culture system, the TH protein expression was highest in the final differentiated stage (Fig. 2; TH). For the tissue samples, the highest TH protein levels were found in the proliferation zone of the cerebral cortex, SVZ, at GW 19 (Fig. 2), consistent with previously published anatomical data [4,6,9]. For the D1 receptor protein, convincing bands were not seen by western blot (Fig. 2), despite using 2 different primary–secondary antibody pairs (not shown). However, we found strong evidence of D5 protein in all 5 stages (Fig. 2; D5), suggesting that hESC line-H9 utilizes DA receptors coupled to the cAMP-stimulating pathway. Western blot using anti-D2 antibody showed one prominent 33 kDa band, with higher signal from the GE than the other brain regions (Fig. 2; D2).

Functional DA receptors

So far, our data suggest the presence of DA receptors in hESC line H9 (Figs. 1 and 2). However, such analyses (rtPCR and western blot) are insufficient to determine the physiological maturity of DA receptors. To explore the functional aspect of dopaminergic signaling in hESC-H9, we combined multisite Ca^{2+} imaging with focal application of drugs. Round-shaped hESC colonies (Fig. 3A; hESC) were loaded with the Ca^{2+} sensitive dye OGB-1 AM and challenged with

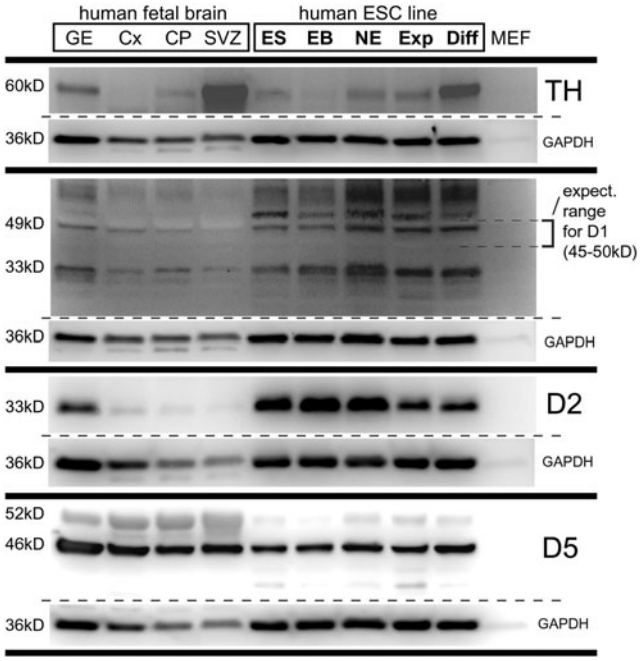

FIG. 2. Western blots of fetal human brain regions and hESC cultures at each stage of in vitro differentiation. Abbreviations: GE, fetal ganglionic eminence (19 gestational weeks [GWs]); Cx, fetal cortex (19 GW); CP, fetal cortical plate (17 GW); SVZ, fetal subventricular zone (17 GW); ES, hESC colonies + MEF feeder layer; EB, embryoid bodies; NE, neuroepithelial colonies; Exp, expansion stage; Diff, differentiation stage; MEF, mouse embryo fibroblast feeder layer. Membranes probed for each of the indicated genes were stripped and reprobed for GAPDH, shown immediately beneath each primary blot. Approximate molecular weights of bands of interest are shown on the *left*. Bracket marks the expected range of D1 receptor band.

brief (≤6 s) iontophoretic drug ejections via glass 15 MΩ micropipettes (Fig. 3A; drug-filled electrode). Brief ejections of ATP (1–3 s) produced Ca^{2+} signals characterized with delayed onset, large amplitude, and duration in all colonies tested ($n = 8$). The signal peaked on average 10 ± 0.9 s after the onset of the iontophoretic pulse (Fig. 3D; ATP). These Ca^{2+} responses persisted in low extracellular Ca^{2+} (0.1 mM, not shown), indicating an involvement of internal Ca^{2+} stores. Calcium transients evoked by D1 receptor agonist SKF38393 (Fig. $3B_1$–B_3) or D2-agonist quinpirole (Fig. $3C_1$–C_3) were notably smaller in amplitude than ATP-evoked transients. The D1-evoked response was on average $11\% \pm 2.6\%$ ($n = 4$), while the D2-evoked response was on average $23\% \pm 5.1\%$ ($n = 9$), compared to the mean ATP-evoked signal. Unlike ATP, SKF and QP did not trigger calcium release in all hESC colonies. The success rate of the QP was 64% (9 out of 14), while the success rate of SKF was only 50% (4 out of 8). In several experiments with iontophoretic application of SKF, especially when the tip of the electrode was closer to the surface of the colony, we observed negative deflections from the signal baseline, suggesting that Ca^{2+} level was transiently decreased during SKF application. A similar decrease in the resting Ca^{2+} level caused by D1 receptor stimulation was found in pyramidal neurons of the rat prefrontal cortex [29]. To evoke calcium signals by SKF or QP, the duration of

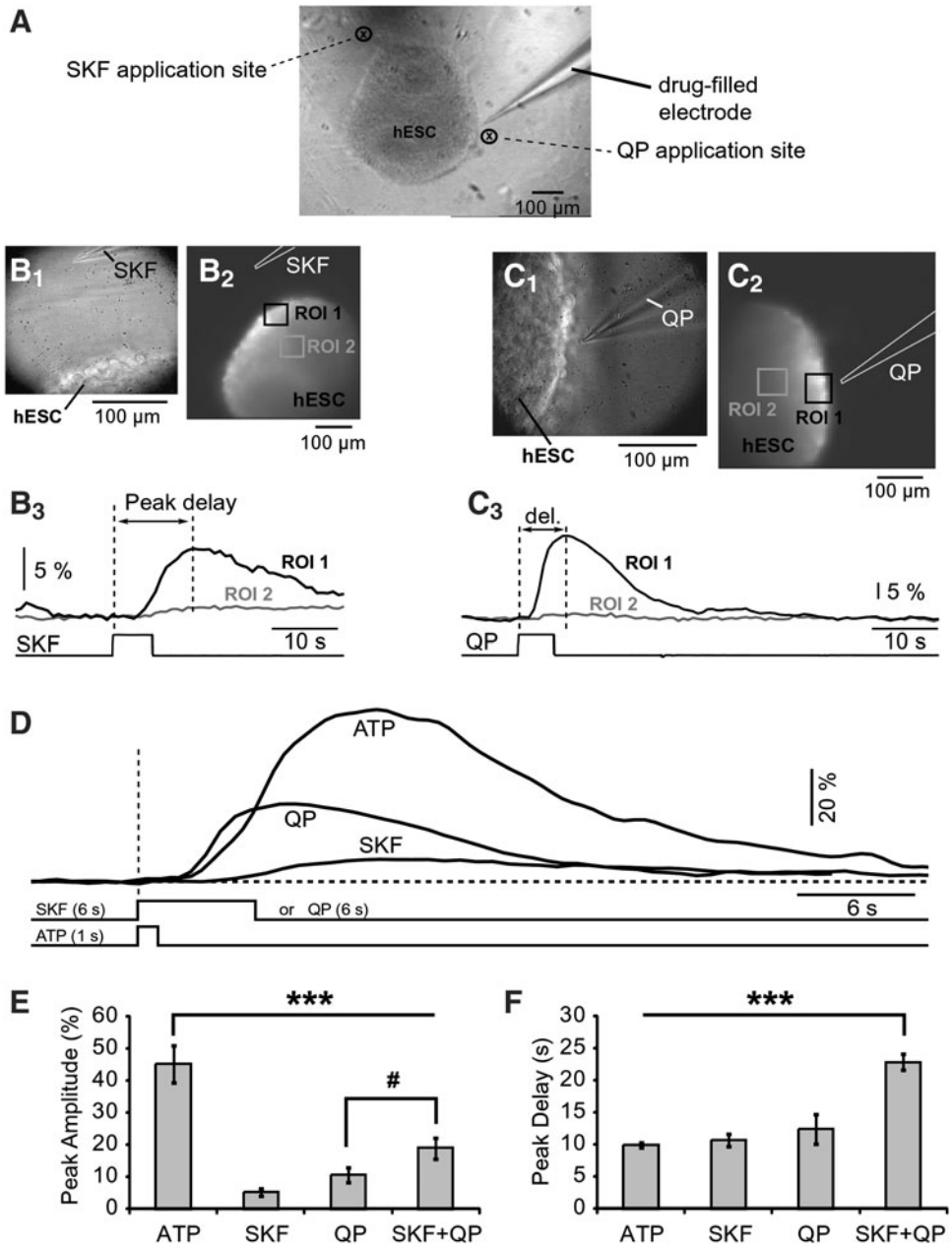

FIG. 3. DA receptor agonists induce internal calcium release in hESC colonies. **(A)** Microphotograph (4× lens) showing iontophoretic micropipette (electrode) positioned next to a hESC colony. **(B_1)** Infrared photograph of the glass electrode and the edge of the hESC colony. **(B_2)** Fluorescent image of an hESC colony loaded with Oregon green 488 Bapta-1. Drawing marks the iontophoretic electrode filled with D1 agonist SKF38393. **(B_3)** SKF-induced calcium transients recorded simultaneously at 2 regions of interest (ROI 1 and ROI 2). Bottom trace depicts time course of the SKF iontophoretic pulse. **(C_1)** Photograph of the QP-filled electrode and the edge of the same hESC colony shown in **(B_1–B_3)**. **(C_2)** Fluorescence image acquired with NeuroCCD. Drawing marks position of the QP electrode (D2 agonist). **(C_3)** QP-induced calcium transients recorded simultaneously at two ROIs (ROI 1 and ROI 2). **(D)** Calcium transients evoked by ATP, SKF, or QP superimposed on the same amplitude and time scale. Each trace is a spatial average of 9–16 pixels. *Vertical dashed line* marks the onset of the drug ejection. **(E)** Peak amplitude of the calcium transient averaged across all successful tests within a group: ATP ($n=8$), SKF ($n=4$), QP ($n=9$), and cocktail SKF+QP ($n=6$). ***ANOVA ($P<0.0001$); #$P>0.05$. **(F)** Same as in **(E)** except time period between stimulus onset and calcium peak was averaged. ***ANOVA ($P<0.0001$).

iontophoretic pulses were increased (up to 6-fold) compared to ATP (Fig. 3D), suggesting that Ca^{2+} release from internal stores were more sensitive to ATP than to DA receptor agonists. The recording sites further away from the drug ejection sites experienced less or no signal (compare ROI 2 and ROI 1 in panels of Fig. 3B and 3C), suggesting that the amplitude of the Ca^{2+} signal followed the diffusion gradient of the drug. To test the hypothesis that D1–D2 receptor heterodimerization causes synergistic potentiation of intracellular Ca^{2+} levels, greater than by activating either receptor

alone [32], we loaded iontophoretic pipettes with both SKF38393 [40 mM] and QP [40 mM]. Six-second-long pulses of the D1–D2 agonist cocktail applied 20–50 μm above the surface of hESC colonies caused calcium transients in 6 out of 9 hESC colonies. The amplitude of the SKF + QP-evoked Ca^{2+} signal was on average 41% ± 7.3% of the mean ATP amplitude ($n = 6$). However, the difference in signal amplitude between SKF + QP and QP alone was not statistically significant (Fig. 3E; #). Interestingly the time delay between stimulus onset (vertical dashed line) and the peak of the Ca^{2+} transient was significantly longer in the SKF + QP group compared to other groups (Fig. 3F; ANOVA, $P < 0.0001$).

Treatments with drugs added in culture media

Taken together, the rtPCR analysis (Fig. 1), western blots (Fig. 2), and drug-induced release from internal calcium stores (Fig. 3) suggest that pluripotent hESC and differentiating hESC colonies express DA receptors and respond to dopaminergic stimulation. The continuous presence of DA receptors throughout 5 stages of the hESC differentiation protocol (Fig. 1A) imposes a great difficulty on researchers who wish to determine the right timing (onset), the right duration, and the right dosage for DA treatment in order to optimize neuronal yield from hESCs. This is further complicated by the existence of multiple dopaminergic pathways (eg, D1 like or D2 like) and synergistic interactions between them. In the remainder of the article we varied the timing of the dopaminergic treatment. DA, or DA receptor agonists and antagonists were introduced in the media at different stages of the dbcAMP-based differentiation protocol. The term "early treatment" indicates treatment applied to Stages 1–3 (undifferentiated hESC, EBs, and neuroepithelial colonies). The term "late treatment" pertains to protocols in which differentiating neurons (Stages 4–5) were treated with dopaminergic drugs, either continuously (24 h) or intermittently (4 h/day, no drug overnight). Controls were treated with water on the same time points.

Early treatment

To assess the effects of DA receptor stimulation (or inhibition) early in the differentiation process, differentiating hESCs were treated with dopaminergic drugs beginning 3 days before EB creation (Day minus 3) and continuing until the end of the neuroepithelial stage at Day 8 (Fig. 4A). In the first experiment of this series hESCs were treated with D1/D5-antagonist SKF83566 [0.5 μM], D2-antagonist L741 [0.5 μM], or DA [10 μM] (Fig. 4C, E; Experiment 1). In the repeated experiment, in addition to the 3 aforementioned drugs, hESC colonies were also treated with D1-agonist, SKF38393 [0.5 μM], or D2-agonist, quinpirole [0.5 μM] (Fig. 4C, E; Experiment 2). When using gross EB morphology and

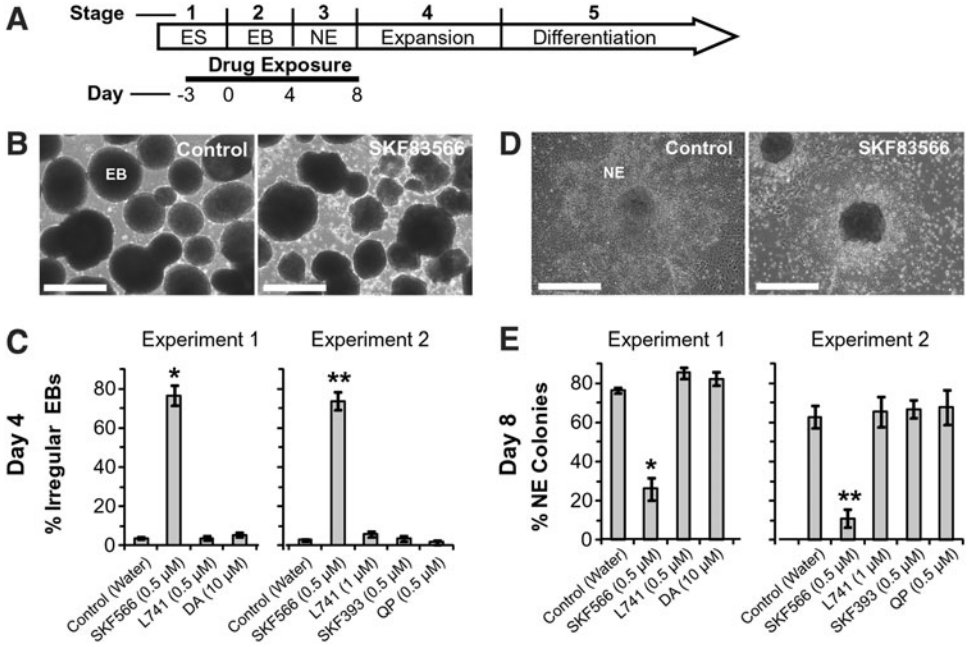

FIG. 4. Effect of dopaminergic drugs on creation of EBs and neural progenitors. **(A)** Time course of the experiment. Normal EBs (Control) and irregular EBs treated with the indicated drugs. **(B)** Normal EBs (*left*) and irregular EBs treated with 0.5 μM SKF83566 (*right*). **(C)** Cultures were exposed to the indicated drugs from days 3 to 8 of our standard differentiation protocol. EBs were scored for normal smooth surface versus irregular surface. 1 and 2 are independent experiments. $n = 2$–3 wells per treatment. Error bars = SEM. Experiment 1: Kruskal–Wallis one-way ANOVA on ranks, $P = 0.018$. For SKF83566 versus control $P < 0.05$ using Dunn's pairwise comparison. Experiment 2: Kruskal–Wallis one-way ANOVA on ranks, $P = 0.007$, for SKF83566 versus control $P < 0.05$ using Dunn's pairwise comparison. The EBs in **(B** and **C)** were seeded to create the colonies in **(D)** and **(E)**. **(D)** Normal neuroepithelial colony (*left*) and non-neuroepithelial colony after treatment with 0.5 μM SKF83566 (*right*). **(E)** Neuroepithelial stage cultures were scored for % neuroepithelial colonies on day 8. For Experiment 1, Kruskal–Wallis one-way ANOVA on ranks $P = 0.011$; Control versus SKF83566 Mann–Whitney Rank sum test $P = 0.029$. For Experiment 2, ANOVA $P < 0.001$; Tukey test on Control versus SKF83566 $P < 0.001$. All scale bars = 500 μm.

% neuroepithelial morphology as endpoints, only SKF83566 caused a statistically significant change compared to controls that received vehicle (Fig. 4C, E; asterisks). Cultures treated with SKF83566 showed rough EB borders, instead of the typical smooth EBs (Fig. 4B). Before creation of EBs, no significant differences in numbers of differentiated hESC colonies were found compared to control wells. More specifically, after 3 days of continuous drug treatment, the mean number of differentiated hESC colonies per well (mean + s.e.m.) were:, Control 10.5 ± 0.7 ($n = 6$), SKF83566 8.3 ± 1.2 ($n = 3$), L741 11 ± 1.5 ($n = 3$), SKF38393 9.3 ± 2.6 ($n = 3$), quinpirole 6 ± 1.5 ($n = 3$). After EBs were seeded and allowed to adhere to the surface of the dish, colonies from SKF83566-treated cultures rarely showed the typical neuroepithelial morphology of elongated cells with neuroepithelial ridges (Fig. 4D; Control). Instead, SKF83566-treated wells were populated by slowly transforming EBs without neuroepithelial skirts around them, suggestive of an apparent stall in neurodifferentiation. Treatment with DA [10 μM], or L741 [0.5 μM], or SKF38393 [0.5 μM], or quinpirole [0.5 μM] had no effect on these two endpoints.

Late treatment

Late treatment (days 14–28) with DA [10 μM] or antagonists (SKF83566 [0.5 μM] or L741 [0.5 μM]) did not produce striking morphological differences (data not shown). In contrast to early treatment (Fig. 4), SKF83566 had no noticeable effect on morphology or density when applied during the differentiation stage (not shown).

Neurites

To examine the formation of neurites, hESC cultures were treated with DA [10 μM] or D1-antagonist SKF83566 [0.5 μM], or D2-antagonist L741 [0.5 μM]. Drug treatments were administered either early (days 3–8) or late in the protocol (days 14–28). In either paradigm, early or late, the neurons were allowed to differentiate 36 days, at which time neurite quantitations were made in these experimental series. Neurites were counted under phase contrast (Fig. 5B, C). The counting was performed blindly, as the experimenter was not aware of the labels. DA [10 μM] applied at the differentiation stages ("Late treatment," days 14–28) was the only treatment to change the number of neurites, producing a ~90% increase in average neurites per field (Fig. 5D, E). These cultures were subsequently extracted for total RNA measurements. Total amounts of RNA obtained for the early treatment groups in this experiment were similar (1.0, 1.1, 0.94, and 1.0 mg for control, DA, SKF566, and L741, respectively) and likewise total amounts of RNA for the late treatments were similar (0.76, 0.92, 0.72, and 0.81 mg for control, DA, SKF566, and L741, respectively), suggesting an absence of large differences in cell density.

Dopaminergic neurons

To further investigate the effects of DA on the production of dopaminergic neurons, we treated differentiating cultures of hESCs with DA and assayed for the dopaminergic neuronal marker TH and pan neuronal marker βIII-tubulin

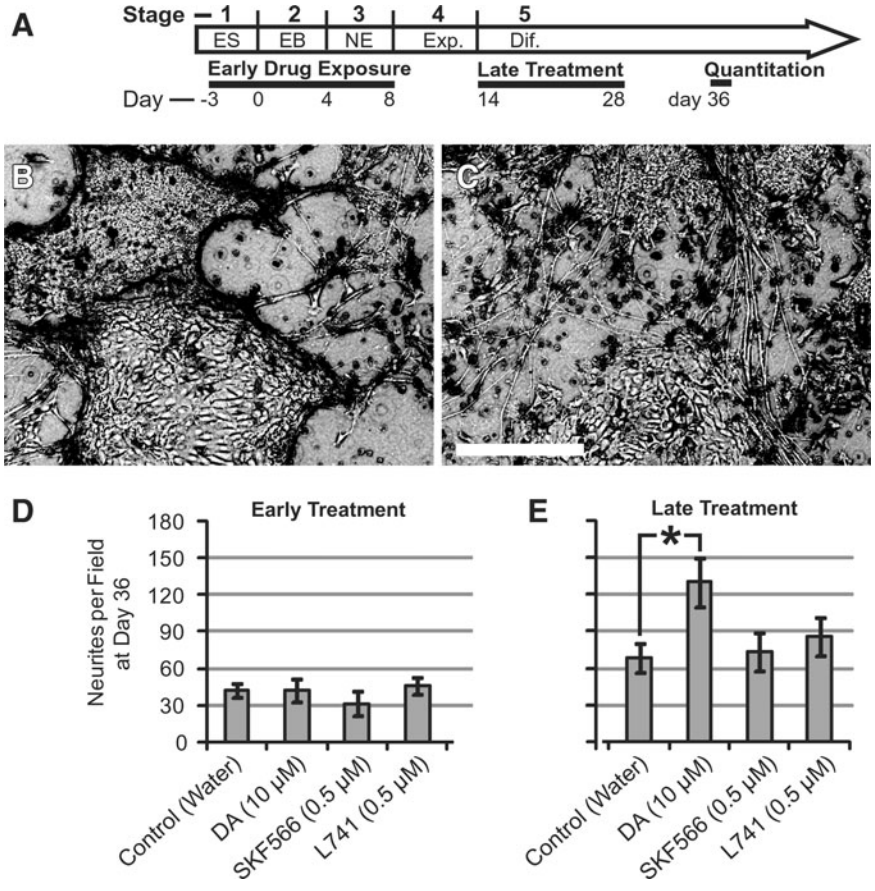

FIG. 5. Effect of DA receptor ligands on neurites. **(A)** Time course of the experiment. Cultures were treated as indicated from days −3 to 8 (early treatment) or from days 14 to 28 (late treatment) of our standard differentiation protocol. All cultures were maintained until day 36 and neurites quantitated. **(B)** Phase-contrast image (inverted) showing neurites in the control well. **(C)** Neurites in wells treated with DA [10 μM]. **(D)** Quantitation of neurites exposed to "early treatment." Scale bar = 500 μm. **(E)** Quantitation of the "late treatment" data. $n = 9$ fields counted per treatment. One-way ANOVA, $P = 0.038$. Tukey test for Control versus DA late treatments $P = 0.045$.

(TUJ1). We hypothesized that early exposure to DA can "prime" the EBs toward more robust proliferation or toward greater commitment of postmitotic neurons to the DA subtype [33]. To test this hypothesis, in the next series of experiments, we introduced DA into the hESC cultures at the very onset of differentiation, during Stage 2 (EB) and Stage 3 (neuroepithelial rosettes). DA treatment was stopped when the rosettes were lifted and reseeded (Fig. 6A; Day 11). Upon reseeding of DA-treated neuroepithelial rosettes (Stage 4) we typically observed 2 characteristics of human cultures. Some regions of the coverslip exhibited non-neuroepithelial morphology (Fig. 6B), while other regions of the same coverslip exhibited neuroepithelial ridges. Both characteristics can be visually identified on an inverted microscope (Fig. 6C; arrows) and used for quantitative comparison between 2 experimental groups (Fig. 6D).

Treatment with 10 μM DA (during Stages 2–3) caused a significant increase (Tukey test, $P < 0.05$, $n = 8$ slips per group) in the number of neuroepithelial colonies midway through Stage 4 (Fig. 6D). Therefore, early treatment with DA (days 1–11) was associated with more neuroepithelial colonies at day 17, during expansion stage, when immature neuroepithelial colony morphology is not expected. The DA exposure may have delayed the expansion caused by the proliferative actions of bFGF, which was present at Stage 4 in both control and test conditions (Fig. 6A). Dual TH-TUJ1 immunofluorescence revealed that early treatment with 10 μM DA potentiated the production of TH^+ clusters by the end of the protocol (Fig. 6E). The numbers of $TUJ1^+$ clusters also increased, indicating that the increase in TH^+ clusters was in large part due to more neurons forming, not direction of a higher proportion of neurons to a dopaminergic fate.

DA versus dbcAMP

Activation of the cAMP/PKA/CREB pathway has been used by several investigators to help differentiate hESCs into DA neurons [22–24]. As expected, dbcAMP treatment during the stage of the protocol (Fig. 7A; Stage 5) caused a statistically significant increase in the number of TH^+ colonies per dish (Fig. 7C; dbcAMP, red column) 83% ± 20% ($n = 16$) compared to no-dbcAMP control (Fig. 7C; Control, $n = 23$). dbcAMP exposure had little effect on overall neuronal differentiation, as assayed by TUJ1 staining and quantification of $TUJ1^+$ clusters (Fig. 7C; green columns); an increase of 13% ± 13% ($n = 16$) was not statistically significant ($P > 0.05$).

Alongside the dbcAMP treatment, DA alone was introduced in the culture media on the first day after reseeding of neuroepithelial rosettes (day 14), and the same drug treatment [DA 1, 10, or 100 μM] was maintained to the end of experiment (Fig. 7A; Stages 4 and 5). To avoid overstimulation of DA receptors or toxic effects of DA degradation products, DA was applied for 4 h every day, and cultures were maintained DA-free overnight. On the 2nd week of Stage 5 (day 36), we examined TH expression, and the pan neuronal marker βIII-tubulin (TUJ1 antibody) using dual

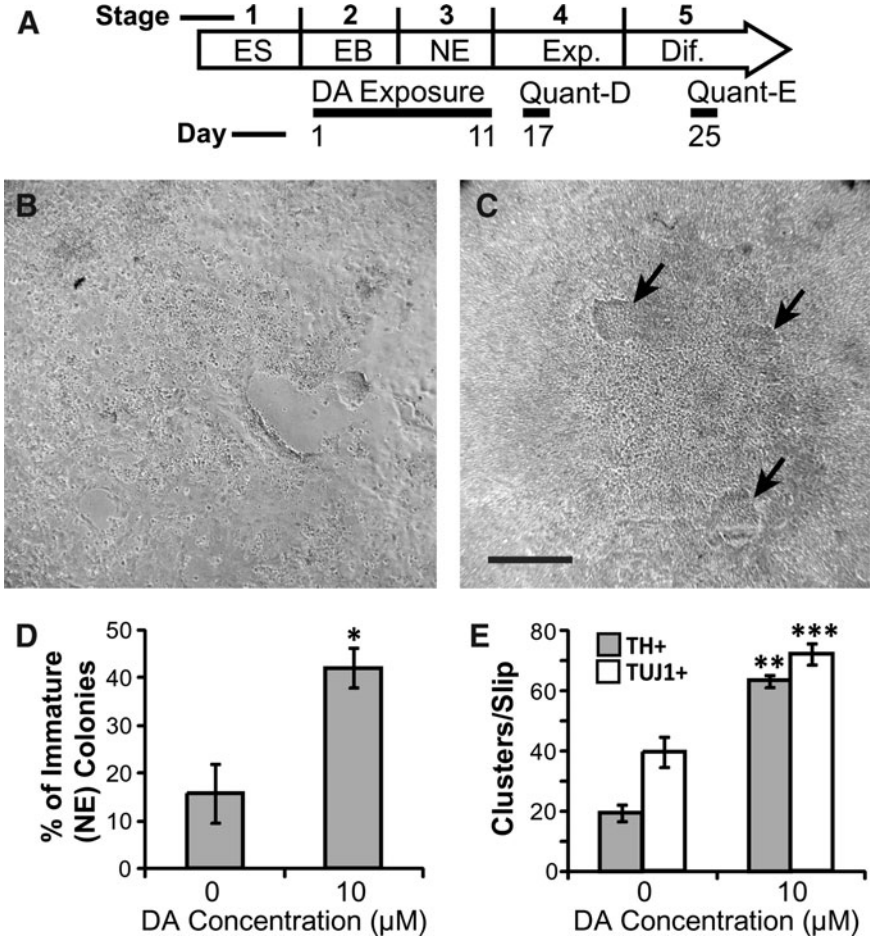

FIG. 6. Effect of early DA treatment on differentiating H9 hESCs. **(A)** Time course of the experiment. Cells were treated with continuous DA during Stages 2–3 (days 1–11) of differentiation. **(B, C)** Phase-contrast images of colonies midway through the differentiation protocol (day 17, Stage 4). **(B)** Colony lacking neuroepithelial morphology. **(C)** Colony displaying primitive neuroepithelial morphology. *Arrows* indicate characteristic ridges between groups of elongated cells not seen in **(B)**. **(D)** Quantitation of morphology midway through the differentiation protocol (day 17, Stage 4), % of colonies with neuroepithelial morphology were determined for each coverslip ($n = 8$ slips per group). **(E)** Quantitation of the number of TH^+ and $TUJ1^+$ clusters per coverslip with early DA treatment. Cells were fixed on day 25 after 7 days in terminal differentiation media. Immunofluorescent staining for TH and TUJ1 was performed. Clusters of 10 or more TH^+ cells and 20 or more $TUJ1^+$ cells were counted. 7–8 slips per group. *Tukey test, $P < 0.05$. **Tukey test, $P < 0.001$. ***t-test $P = 0.0002$. Error bars = SEM.

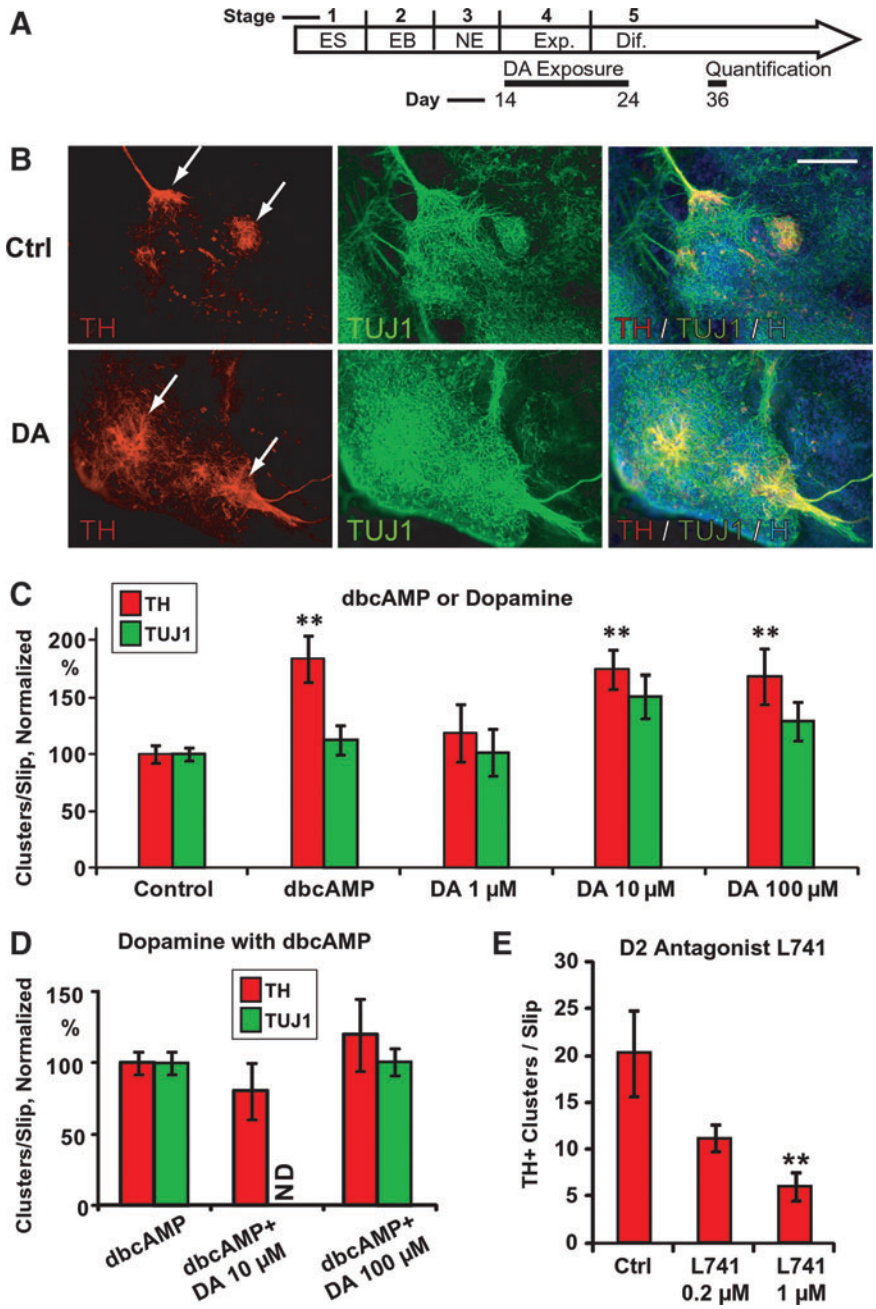

FIG. 7. DA influences differentiation of H9 hESCs. **(A)** Time course of the experiment. **(B)** 10× images of immunostained colonies, control or 100 µM DA; TH, tyrosine hydroxylase; TUJ1, βIII-tubulin; H, Hoechst. Scale bar = 200 µm. **(C)** Quantitation of number of TH^+ or $TUJ1^+$ clusters per coverslip after differentiation of H9 hESCs to neurons. Wherever indicated, cells were exposed for 7 days to 1 mM dbcAMP during Stage 5. Cells were exposed to intermittent DA (3–4 h/day) during Stages 4–5 as indicated in **(A)**. Immunofluorescent staining was performed after 7 days in Stage 5 for TH and TUJ1, and clusters of stained cells quantitated. *Arrows* indicate individual clusters of TH^+ cells. Data were combined from 4 independent replicate experiments. 8–23 coverslips per group. For TH: 100% = 11.9 clusters/slip; Kruskal–Wallis one-way ANOVA on Ranks $P = 0.001$; **Mann–Whitney rank-sum pairwise tests: TH control versus dcAMP $P < 0.001$; TH control versus 10 DA $P < 0.001$; TH control versus 100 DA $P = 0.009$. TUJ1 groups show no significant differences. For TUJ1: 100% = 32.6 clusters/slip. **(D)** Lack of additive effect of dbcAMP and DA. 1 mM dbcAMP was added continuously to the cultures during Stage 5. The indicated concentrations of DA were added during Stages 4–5 (intermittently, drug-free nights). No significant differences between groups. The data in **(D)** are combined from 3 independent experiments. $n = 4$–17 slips. ND, not determined. **(E)** Inhibition of DA neurogenesis by D2 receptor antagonist L741. The indicated concentrations of L741 were added intermittently during Stages 4–5. For **(E)**: one-way ANOVA $P = 0.002$. Tukey test; control versus 1 µM L741, $P = 0.007$. Color images available online at www.liebertpub.com/scd

immunofluorescence. Consistent with the previous report, the dbcAMP differentiation protocol produced large clusters of neurons containing smaller clusters of TH^+ neurons [21]. In some cases, one tangled mass of $TUJ1^+$ neurons contained 2 or 3 clusters of putative DA cells (Fig. 7B; arrows). Occasionally, isolated TH^+ neurons (putative DA neurons) were found outside neuronal clusters, but the overwhelming majority of TH^+ neurons were lumped together in several distinct spots on the bottom of the dish (Fig. 7B; arrows). Clusters containing 10 or more TH^+ cells were included in the data analysis and counted for comparison between groups.

In the DA-treated groups [10 and 100 µM], we found a significant increase in the number of TH^+ clusters per coverslip compared to drug-free control (Fig. 7C; red columns, 74% ± 17% [$n = 9$ slips] and 68% ± 24% [$n = 10$ slips], respectively). DA exposure in the last 2 stages of the differentiation protocol did not significantly influence the total number of neuronal clusters. Even though there was no significant difference in number of $TUJ1^+$ clusters between controls and DA treatment, there was a trend for the numbers of $TUJ1^+$ clusters to increase in parallel with the increase in TH^+ clusters (Fig. 7C; green columns).

To determine whether the size of the clusters changed under the DA treatment, microphotographs were taken of TH^+ clusters with a 10× objective lens and fluorescent signals quantified. There was no difference in TH^+ signal (integrated optical densities) between controls ($n = 44$ pictures) and the 100 µM DA group ($n = 43$ pictures, data not shown). The average TH intensity at 100 µM DA was found to be

95% ± 11% of the control, indicating that the DA treatment did not increase the size of the TH^+ cell clusters. DA-treated clusters contained similar number of TH^+ neurons as controls. The ratios of TH fluorescent signal to TUJ1 fluorescent signal (red/green) were also identical between controls and 100 μM DA, the latter found to be 97% ± 11% of the control ratio (data not shown). Mean areas of the TH^+ clusters were not significantly different (data not shown) although the 100 μM DA group mean was 18% larger than the control group mean.

DA together with dbcAMP

To examine the signal transduction pathway involved in the increase in TH^+ cells induced by DA, cells were treated with DA [10 or 100 μM] and 1 mM dbcAMP simultaneously. The concentration of dbcAMP used has been shown to be maximally stimulative in neurodifferentiation protocols [34,35]. Two DA concentrations, 10 and 100 μM, were combined with dbcAMP. Although the two DA concentrations [10 and 100 μM] caused a significant increase in TH^+ clusters per dish when applied on their own (Fig. 7C), in combination with dbcAMP (Fig. 7D), they had no additive effect. In other words, we did not detect any significant changes in the count of TH^+ clusters when DA + dbcAMP groups were compared to dbcAMP alone (Fig. 7D).

Selective D2-like DA receptor inhibition

So far our experiments established that DA receptor stimulation improves the yield of hESC-derived DA neurons via a positive regulation of cAMP (Fig. 7C, D). However, D2-like receptors, which are inhibitors of cAMP, were expressed in late stages of hESC neurodifferentiation (Figs. 1 and 2). To address the impact of D2-like DA receptors on the production of DA neurons from hESCs the expanding neuroepithelial rosettes were treated with D2-antagonist L741 [36] late in the protocol, when TH protein is expressed (Fig. 2). The L741 treatment applied at differentiation stages (Stages 4–5) produced a dose-dependent decrease in TH^+ clusters, inconsistent with the involvement of cAMP/PKA pathway in potentiating numbers of TH^+ cells (Fig. 7D, E). However, the attenuation of TH^+ cells by a D2/3/4 antagonist is consistent with reports that D2 and D3 receptors are coupled to ERK, and with reports that D2-agonists promote DA neuron development through the ERK pathway instead of by modulating cAMP [33,37]. We note that in this experiment the DMSO vehicle-treated controls (Fig. 7E; Ctrl) showed higher numbers of TH^+ clusters than normally found in DMSO-free controls, consistent with reports that DMSO induces differentiation of neuroblastoma lines and stem cells [38,39].

Physiological properties after DA treatment

So far, we have established that stimulation of DA receptors during neurodifferentiation of hESC cultures produced a significantly greater number of DA neuron clusters, compared to cultures maintained in regular (Control) media (Fig. 7C). Next, we asked whether the increase in neuron clusters was at the expense of neuronal physiological maturity. Our working hypothesis stated that facilitated neuroproliferation and *en masse* commitment to dopaminergic neuron type leaves neurons with less time and resources to build fully excitable membranes capable of AP generation. In the human fetus (16–21 GWs), the postmitotic neurons mature gradually by inserting voltage-gated sodium channels into the plasmalemma, by decreasing their electrical input resistance, and by making their resting membrane potential more and more negative as neural maturation progresses [28]. The insertion of sodium channels in developing human neurons is manifested in electrophysiological recordings by an increase in peak amplitude of the fast inactivating sodium current paralleled by neuronal ability to generate APs [28]. In the current project, whole cell recordings were performed on differentiated cells at Stage 5 (days 22–38), after at least 2 weeks of chronic DA exposure. Each cell was typically recorded in 2 electrical configurations; current clamp for assessing the voltage waveforms of APs (Fig. 8A), and voltage clamp for assessing neural transmembrane currents: inward sodium current (Fig. 8B) and outward potassium current (not shown). The electrophysiological properties of hESC-derived neurons were not comparable to the mature neurons in mammalian brain. For example, mature neurons in rat brain slice (neocortex) have several fold greater amplitude of sodium current, much narrower AP waveforms, and greater ability to sustain repetitive AP firing without the loss of AP amplitude [29]. The small-size Na^+ current, broad APs, and relatively weak repetitive AP firing (Fig. 8) are characteristics of postmitotic neurons found in the intermediate zone (migratory zone) and the cortical plate (differentiation zone) of the human fetal cortex in the 2nd trimester of gestation [28].

To assess the influence of exogenous DA exposure on the electrical properties of the hESC-derived neurons, 4 physiological parameters: (1) resting membrane potential (V_r), (2) input resistance (R_{in}), (3) peak sodium current (I_{Na}), and (4) peak potassium current (I_K), were compared across 3 experimental conditions: 0 μM DA ($n = 30$), 10 μM DA ($n = 18$), and 100 μM DA ($n = 8$ neurons). Both, the mean V_r and mean R_{in} were similar in all 3 conditions (Fig. 8C), indicating that DA did not affect passive membrane parameters in developing human neurons. Whole cell recordings detected a trend of increasing Na^+ and K^+ voltage-dependent currents with an increase in DA concentration (Fig. 8C). Larger Na^+ and K^+ current would be consistent with more robust and mature neurons; however, statistical significance was not achieved (Fig. 8C). Twenty-one percent ($n = 30$) of patched cells without exogenous DA exposure displayed APs, while in the 10 μM DA group 38% ($n = 18$) of the cells displayed APs (not significantly different). Taken together, the electrophysiological measurements of V_r, R_{in}, Na^+, and K^+ currents failed to detect any statistically significant changes in neuronal functional properties upon chronic (2 weeks) treatment with DA. When cells with zero Na^+ current (which are potentially non-neuronal cells) were removed from the analysis, there continued to be no significant differences between groups (data not shown).

Expression of neuron-specific markers upon drug treatment

hESC cultures were treated with drugs either early or late in the protocol (Fig. 9A). At day 36, we collected differentiating neurons and examined mRNA expression by rtPCR and qPCR for evidence that treatment with dopaminergic

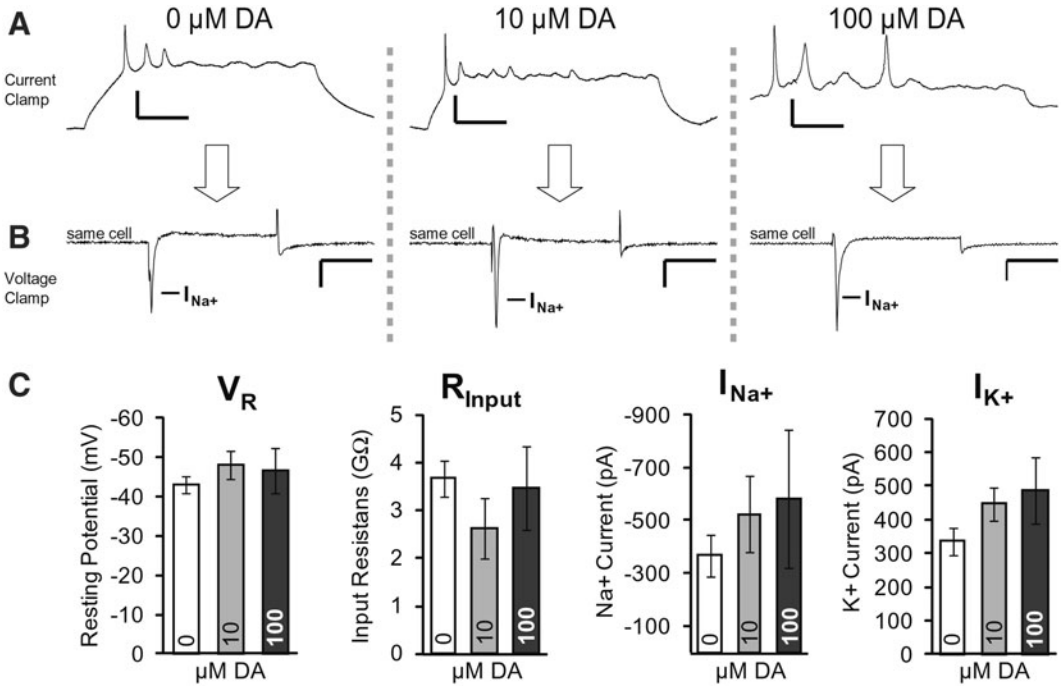

FIG. 8. Electrophysiological parameters of the neurons derived with or without DA. **(A)** Representative traces of 3 cells in current clamp exposed to 0, 10, or 100 μM DA. Vertical scale bar = 20 mV, horizontal scale bar = 20 ms. **(B)** Corresponding traces of the same 3 cells in voltage clamp. Vertical scale bar = 200 pA, horizontal scale bar = 20 ms. **(C)** Peak Na+ current, peak K+ current, input resistance, and resting membrane potential, for 0, 10, and 100 μM DA-treated hESCs. Cells were patched between days 22 and 38 of the protocol. $n = 30$, 18, and 8 for 0, 10, and 100 μM, respectively. Error bars = SEM.

drugs cause a change in lineage or neural subtype. mRNA for the neuroectodermal marker *PAX6* was expressed in all regions of the human fetal brain (Fig. 9B). In hESC cultures the *PAX6* expression was highest at the NE stage (Fig. 9C; NE). Despite the change in morphology of EBs and subsequent neuroepithelial colony appearance (Fig. 4), we saw no change in *PAX6* mRNA levels in cultures treated with SKF83566, assayed at the end of the neuroepithelial stage, day 8 (Fig. 9D). A temporal analysis across the stages of differentiation indicated that the midbrain markers *GIRK2* and *LMX1A* had the highest expression at Stage 5, while *MSX1* had the highest expression at Stage 4 (Fig. 9C; Exp.). mRNA for these 3 midbrain markers and the additional neuronal markers *VGLUT1* (glutamatergic), *GAD1* (GABAergic), and *βIII-Tub* (pan neuronal) were also measured after 36 days of differentiation with either early or late drug treatments. These cultures were the same used in Fig. 5. Each result was normalized to the level of the housekeeping gene, *ACTB*, in the corresponding culture sample (Fig. $9E_1$). Interestingly, in this experimental series all drug treatments caused a notable decrease in *VGLUT1* and *GAD1*, accompanied by a small decrease in *βIII-Tub* (Fig. $9E_2$–E_4). All drug treatments, except early SKF83566, caused a general decrease in the midbrain markers *GIRK2*, *LMX1A*, and *MSX1* (Fig. $9E_5$–E_7). The late treatment with D2-antagonist L741 also failed to reduce *MSX1* level (Fig. $9E_7$). Response to drug treatment was similar for *VGLUT1* and *GAD1*, while the 3 midbrain markers (*GIRK2*, *LMX1A*, and *MSX1*) formed a separate group, which responded to drugs with a similar profile of mRNA expression (Fig. 9). Expression profiles of *VGLUT1* and *GAD1* had a strong correlation (Pearson's $r = 0.97$), while there was a moderate correlation between midbrain marker expression profiles (*LMX1A*:*GIRK2* $r = 0.85$; *LMX1A*:*MSX1* $r = 0.69$; *GIRK2*:*MSX1* $r = 0.61$).

PA6 coculture

Differentiation of human stem cells into DA neurons is a central topic in the cell replacement therapy, and therefore, many protocols for the differentiation of hESCs into DA neurons have already been designed [40–45]. These protocols can be divided into 2 broad groups: those using specific mouse stromal lines to induce differentiation or those using specific media additives. All of the experiments described in the present study, so far, belonged to differentiation protocols based on media additives. We felt that it was necessary to investigate DA's potential to improve yield of human DA neurons grown on a stromal line. Toward this aim, H9 hESCs were seeded on proliferating PA6 feeder layers. Four DA concentrations (0, 1, 10, and 100 μM) were added to the culture media. All 4 groups were fixed after 14 days of growth and double TH/TUJ1 immunostainings were performed (Fig. 10A, B), as also described in Fig. 7B. We found no significant differences in total number of TH^+ clusters per well (Fig. 10C), but the ratio between TH and TUJ1 integrated density at 100 μM DA was statistically different from control wells [0 μM DA] (Fig. 10D). These results suggest that the PA6 cells produce factors which predominate over any DA activated signal transduction pathways in regards to commitment, differentiation, or survival of DA neurons, but that DA can still activate G_s and the resulting cAMP can increase expression of TH.

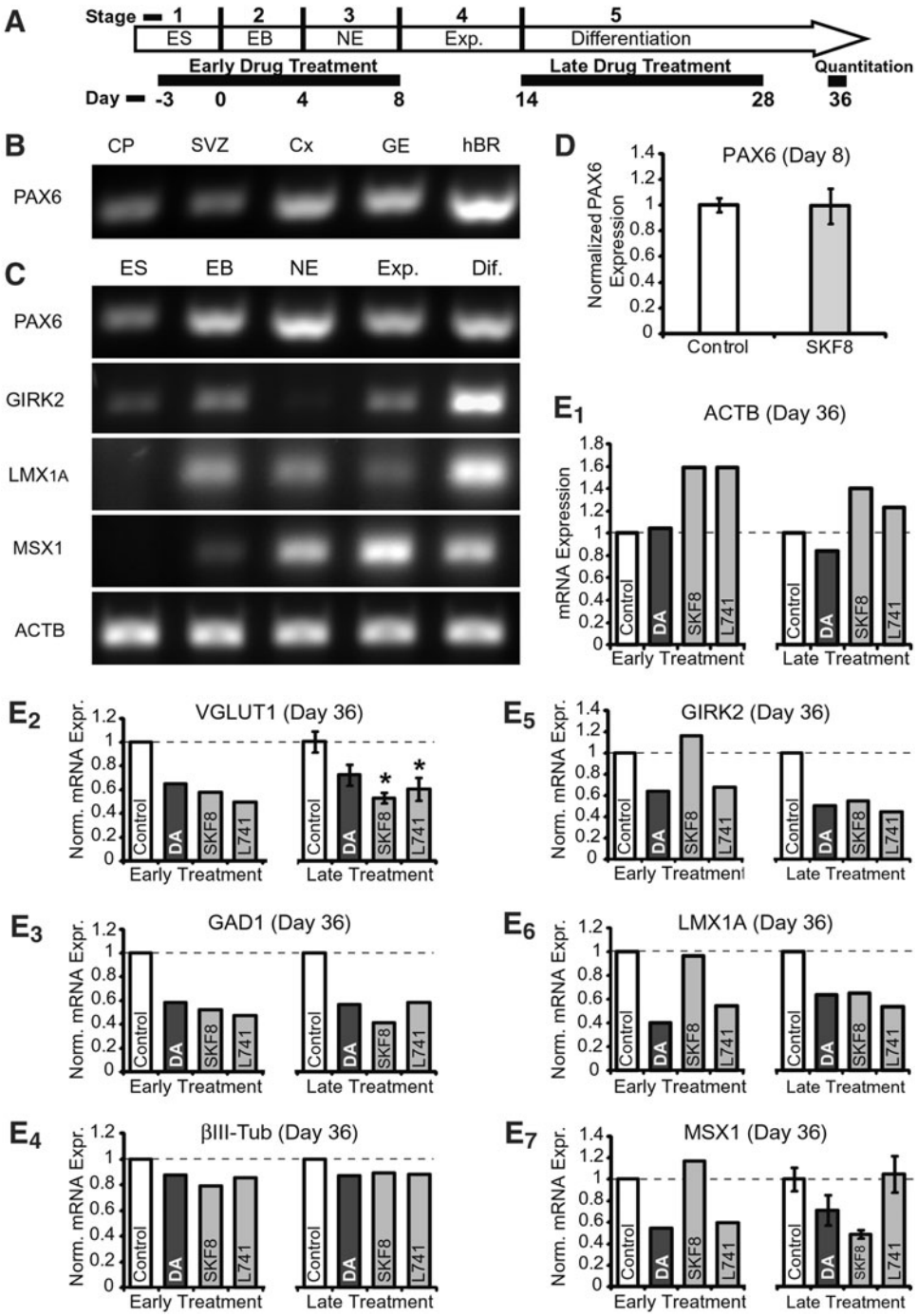

FIG. 9. Midbrain neuron markers upon early or late treatment with dopaminergic drugs. **(A)** Time course of the differentiation protocol showing treatment with DA, D1 antagonist SKF83566 [0.5 μM] (SKF8), D2 antagonist L741 [0.5 μM]. mRNA was extracted at 36 days (quantification), except for *panel* **(D)**, where extraction was done on day 8. **(B)** rtPCR of *PAX6* in human fetal brain tissue samples (CP, SVZ, Cx, and GE) and adult brain (hBR). **(C)** rtPCR of *PAX6*, 3 midbrain markers, and housekeeping gene *ACTB* during each differentiation stage. **(D)** qPCR of *PAX6* in neuroepithelial colonies (control $n=14$; SKF83566 $n=7$). **(E)** qPCR of housekeeping gene (*ACTB*), neuronal markers (*VGLUT1*, *GAD1*, and *βIII-Tub*), and midbrain markers (*GIRK2*, *LMX1A*, and *MSX1*), in early and late treated cells. PCRs for *VGLUT1* and *MSX1* late treatment were repeated 4 times and the results averaged. Asterisks indicate significant reduction. Post hoc Tukey tests (SKF83566 $P<0.01$) and (L741 $P<0.05$). In *panel* **(E_7)** one-way ANOVA ($P<0.05$), but post hoc Tukey tests did not reveal any differences to the control group (for columns with error bars, $n=4$).

Discussion

We used rtPCR, western blot, multisite calcium imaging, immunostainings, and patch clamp recordings to examine whether stimulation of dopaminergic receptors can be used to improve protocols for in vitro production of human dopaminergic neurons.

DA receptor mRNA in hESCs undergoing differentiation

In the first arm of this study we characterized the expression pattern of 5 DA receptor subtypes (D1–D5). We found that starting from the pluripotent stem cell stage (hESCs, Stage-1) DA receptor mRNA and protein were present throughout the entire neurodifferentiation process; at all 5 stages of the dbcAMP-based differentiation protocol [22]. Expression levels of DA receptor mRNA, suggest that D2-like receptors (D2, D3, and D4) predominate in vitro, especially in the initial ESCs (Stage 1) and the earliest stages of neurodifferentiation (Stages 2 and 3). D1 receptor mRNA is much more abundant in the GE of the human fetal brain than in our cultures (Fig. $1B_1$; D1). Systematic sampling of mRNA through 5 consecutive stages of stem cell differentiation revealed highly dynamic transcriptional regulation. For example, D5 and D3 messages peaked in undifferentiated

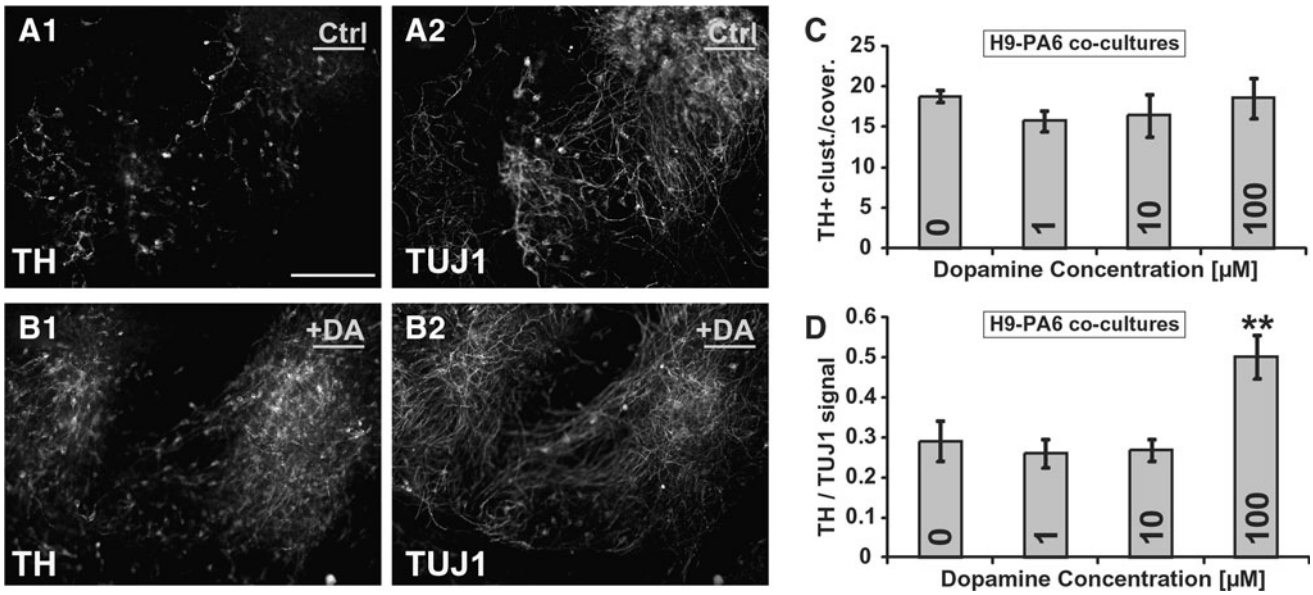

FIG. 10. Effect of DA on H9 differentiation in PA6 coculture. H9 cells were seeded on PA6 feeder layers and exposed to the indicated concentrations of DA continuously. Cells were fixed on day 14, and dual immunofluorescent staining for TH and TUJ1 was performed. **(A1, A2)** 0 DA: TH, TUJ1 staining. **(B1, B2)** 100 μM DA: TH and TUJ1 staining. Scale bar = 200 μm. **(C)** The 3 brightest TH fields were photographed per coverslip. Signal intensities were quantitated. Ratio of total TH signal/TUJ1 signal was calculated. **Kruskal–Wallis one-way analysis of variance on Ranks $P = 0.002$. **(D)** Number of TH^+ clusters of cells per coverslip. $n = 4$–5 coverslips per group. Error bars = SEM.

hESCs (Fig. $1B_2$), while D4 and D2 peaks occurred in the 3rd and 4th stage, respectively. Three lines of evidence confirm the good quality of the rtPCR data. First, the expression level of *ACTB* was stable in all samples (Fig. $1B_2$; ACTB). Second, the highest level of TH expression was detected in the most differentiated neuronal stage (Stage 5), when dopaminergic neurons appear in response to dbcAMP [21,22]. Third, DA receptor subtypes were detected in all differentiation stages, consistent with the published data on sustained and abundant DA receptor gene expression, predominantly in germinative neuroepithelial zones. Previous reports have shown that D1, D4, and D5 message is expressed in human neural progenitors, while human EBs, but not hESCs, have been shown to express D1 mRNA [46,47]. In addition, mouse ESCs have been shown to express D1 and D2 receptors [48]. In rat embryos, D1 and D2 receptors are found in the striatum at least by E14 [49]. Also in rat, D3 receptor is expressed at day E14, and is associated with proliferative zones during prenatal ontogeny, whereas the D1 and D2 mRNAs appear mostly in differentiating neurons [50]. We performed a sequential analysis of DA receptor mRNA expression during 5 stages of neurodifferentiation (Fig. 1A), and found more expression of the inhibitory D2, D3, and D4 messages in comparison to the stimulatory D1 and D5 (Fig. 1B). Therefore, the result in Fig. 6, where early treatment of differentiating stems cells led to more neurons, is consistent with previous reports, where activation of D2 and D3 leads to increased proliferation [7,51–53], but see Ref. [54]. In the present study, mRNA for the D3 receptor showed the highest expression in Stage 1, when hESCs were maintained in an undifferentiated state (Fig. 1B). This finding is consistent with reports that in adult rats, a 10-fold increase of proliferating cells in the neostriatum has been observed upon stimulation with a D3 agonist [52,55].

DA receptor proteins in hESCs undergoing differentiation

The presence of D2 and D5 receptor protein in differentiating hESCs was confirmed in western blot (Fig. 2). As expected from the relatively low expression of D1 mRNA (Fig. 1), convincing bands were not seen by western blot, in spite of using 2 different primary–secondary antibody pairs. Both antibody pairs detected a faint 33 kDa band (Fig. 2; D1). Another caveat of our protein assay pertains to D2 subfamily. Western blot using anti-D2 antibody showed one prominent 33 kDa band (Fig. 2; D2). Although bands of 48 and 70 kDa are normally associated with D2, a 33 kDa D2-receptor band has also been reported [56], as well as a 37 kDa doublet [57]. The apparent molecular weight variability of D2 protein is due to cleavage, glycosylation, palmitoylation, and phosphorylation status of D2 protein [58]. Between 5 stages of hESC neurodifferentiation (Fig. 1A), the TH protein expression was highest in the final differentiated stage (Fig. 2; TH, Stage 5), consistent with the previously published dbcAMP–induced boosting of TH in hESCs [21,22]. For the fetal brain samples, highest TH protein levels were found in the proliferation zone of the cerebral cortex, SVZ (Fig. 2), consistent with the published anatomical data [4,9]. The next highest TH band in the fetal brain was detected in GE, consistent with the presence of DA neurons in the gangliothalamic body [49,51,55].

The DA receptor mRNA (Fig. 1) and DA receptor protein expression (Fig. 2) were measured at all 5 stages of H9 neurodifferentiation, which allowed us to make direct comparisons between 2 data sets. Highest TH protein levels were found in the most differentiated stage (Stage 5), consistent with our mRNA data (Fig. 1). D1 receptor protein was not found, consistent with the lack of mRNA (Fig. 1). D2 and D5-

receptor proteins were detected in all 5 stages (Fig. 2), as previously shown for the mRNA (Fig. 1). However, some discrepancies between RNA and protein data were observed for D2 and D5. For example, D5 RNA attenuated with stage progression (Fig. 1), while protein remained relatively stable in the same phase of in vitro experiment (Fig. 2).

There are 2 possible explanations for discrepancies between RNA and protein (Figs. 1 and 2). In regard to postmortem fetal tissue, the RNA and protein extractions were done on separate sections harvested from the same block of brain. It is possible that sections contained variable thickness of major cortical zones [SVZ, intermediate zone (IZ), and CP] either due to natural anatomical variation or due to the cutting artifact. A similar problem exists with culture samples, because RNA and protein were not extracted on the same round of differentiation. A more likely explanation for discrepancies between RNA and protein in our measurements (Figs. 1 and 2) is post-translational regulation of DA receptor protein expression. Published literature frequently show lack of association between DA receptor mRNA and DA receptor protein [59–61].

DA receptor signaling in hESC colonies

The functionality of DA receptors was tested using Ca^{2+} imaging because hESCs respond to a variety of agents with intracellular Ca^{2+} release [62]. It has been shown previously that in response to D2 receptor agonist (quinpirole) the undifferentiated hESCs mobilized calcium from intracellular stores [63]. We confirmed the findings of Malmersjo et al. [63] in respect to quinpirole, and we provided new evidence that D1-agonist SKF38393 can be an equally successful trigger of the internal release in hESCs. It is worth emphasizing several important aspects of our calcium imaging experiments. All measurements were performed on typical round-shaped hESC colonies with well-defined edges (Fig. 3A). In the past, dopaminergic drugs were typically applied in the bath [63]. Bath application of dopaminergic drugs is unlikely to mimic the physiology of the DA release (discussed in Ref. [29]). In contrast, we used iontophoretic ejection of DA agonists, which revealed the actual period of time required for the mobilization of calcium ions from the internal stores (Fig. 3B, C; Peak delay). The experimental design based on the iontophoretic application of DA agonists allowed us to determine that the same hESC colony was responding to both SKF and QP stimulation ($n=2$ colonies). Further, in our experiments, only stem cells closest to the source of the drug (closest to the tip of drug-filled pipette) gave the physiological response (compare ROI 1 to ROI 2), indicating that strong dopaminergic stimuli are necessary for the activation of internal calcium stores. The amplitude of the DA receptor-induced Ca^{2+} release was significantly smaller compared to that evoked by ATP (Fig. 3E). These last 2 lines of evidence, requirement for a high concentration of agonist and the small amplitude of the evoked signal, suggest that mobilization of Ca^{2+} from internal stores is not the primary role of DA signaling in hESCs. If D1–D2 receptor heterodimerization amplifies the release of Ca^{2+} [32], then one would expect that a cocktail consisting of potent D1- and D2-like agonists would trigger faster and stronger releases than by either selective agonist alone. However, this was not the case. The amplitudes of SKF+QP signals were not statistically different than QP alone (Fig. 3E). Instead of being faster, the SKF+QP signals peaked significantly later than signals in all other groups (Fig. 3F).

Rational for adding DA to the hESC neurodifferentiation protocol

DA has been found to regulate neuronal proliferation and differentiation via DA receptors [64,65]. More importantly, DA receptors have been theorized to play a critical role in the development of midbrain dopaminergic neurons [33,66] tempting us to speculate that DA may be able to boost the production of dopaminergic neurons from hESCs. This central hypothesis was difficult to test for 2 reasons. First, DA receptors are present in all stages (Figs. 1–3); therefore, dopaminergic treatments should be tested at various time points during the full course of the differentiation protocol (Fig. 1A; Stages 1–5). Second, the 5 well-established DA receptor subtypes and the products of their heterodimerizations [32] point to a plethora of intracellular pathways that can potentially be manipulated by conditioning the culture media. For example, both D1-like [65] and D-2 like receptors [66] affect neuronal development. Also, dopaminergic signals can be manipulated by turning them ON or OFF. For example, the D5 receptor is known for its constitutive activity [67]. In the present study, we tackled the first problem (timing) by exposing hESCs to dopaminergic treatments very early or very late in the course of neurodifferentiation. The second problem (receptor subtype) was addressed by systematic administration of agonists and antagonists.

Neuronal subtypes

Due to the striking effect of the D1/5 receptor antagonist SKF83566 on the morphology of EBs and on neuroepithelial colonies (Fig. 4), we assayed for changes in the mRNA expression levels of *PAX6*, a transcription factor necessary for neuroectodermal fate of neuroepithelial cells [68]. However, we found no difference in *PAX6* mRNA levels in control versus SKF83566-treated Stage 3 (neuroepithelial) cultures (treatment from day 3 to 8, assayed on day 8; Fig. 9D). Consistent with the unchanged expression of *PAX6*, there was no striking decrease in numbers of neurites after 5 weeks of differentiation with either early or late treatment with SKF83566 (Fig. 5D, E). We assayed several markers for neuronal development and found the expected temporal patterns of mRNA expression, with *PAX6* expression greatest at the NE stage, and the midbrain markers *GIRK2*, *LMX1A*, and *MSX1* generally higher toward the end of the protocol (Fig. 9C). To determine whether treatment with dopaminergic drugs (Figs. 4–8) promotes different DA neuronal subtypes, such as midbrain A9 or A10, or nonmidbrain DA neurons [69], we analyzed expression of 3 midbrain markers (*GIRK2*, *LMX1A*, and *MSX1*). We also examined mRNA for 2 commonly used markers, *VGLUT1* (glutamatergic neurons) and *GAD1* (GABAergic neurons) to look for treatment-induced changes in neuronal subtype. Our data suggest that the treatments either reduce differentiation into mature neurons expressing subtype markers, or push the neurons into subtypes expressing other markers. For neurons subjected to 5 weeks of differentiation that were treated continuously with DA or DA antagonists either from day 3

to 8 (Early), or from day 14 to 28 (Late), we see a general decrease in mRNA for 2 neuronal markers at day 36, regardless of the treatment (Fig. $9E_2$, E_3). Because strong expression of *VGLUT1* and *GAD1* are features of neurons incorporated in neuronal networks and engaged in mature forms of synaptic transmission, the PCR data suggested that all treatments reduced the final number of mature neurons on the dish. In the same experiment, we also assayed for the early neuronal marker class III beta-tubulin (*βIII-Tubulin*), and found small decreases in mRNA level (Fig. $9E_4$), suggesting that the total number of neurons did decrease, but not to the same extent as mature glutamatergic and GABAergic nerve cells. Midbrain markers are also likely to reach greater expression level in mature neurons compared to young postmitotic neurons and neuroprogenitors. The small changes in *βIII-Tubulin* and large drop in midbrain markers for all treatments except early SKF8356 (Fig. $9E_5$–E_7), support the idea that drug treatments delayed neuronal maturation. A correlation between the relative expression profiles of all 3 midbrain markers in the range from 0.61 to 0.85 is consistent with coregulation of these midbrain markers. However, we also found a striking correlation between expression profiles of *VGLUT1* and *GAD1* ($r = 0.97$), which are not expected to be coregulated, suggesting that the correlations are due to overall decrease in total numbers of mature neurons in the treatment groups. Although DA increases TH expression according to immunostaining (Fig. 7), we find no evidence that stimulation of DA receptors by DA [10 μM] or blockade of D2 receptors by or L741 [0.5 μM] increase midbrain neuron numbers specifically. The most surprising outcome of midbrain marker analysis involved hESC cultures exposed to D1/D5 antagonist SKF83566. Early (but not late) treatment with SKF83566 [0.5 μM] did not cause any loss of midbrain markers (Fig. $9E_5$–E_7; Early Treatment). In the SKF83566 group, two midbrain markers (*GIRK2* and *MSX1*) were slightly higher than the drug-free controls (Fig. $9E_5$, E_7; dashed lines). The finding that the D5 receptor dominates over the D1 receptor in our hESC cultures (Figs. 1 and 2), combined with the results of the SKF83566 treatments shown in Figs. 4, 5, and 9, where EB morphology is disrupted, yet neurons still form, suggest that constitutive activity of the D5 receptor [67] in the early stages of the protocol is necessary for smooth outer endoderm development on the exterior of the EB. Maye et al. have reported that forskolin treatment of EBs modulates outer endoderm development [70], and our result is consistent with this report, in that, SKF83566 may reduce cAMP by inhibiting constitutive D5-receptor activity; thus, affecting the outer endoderm and resulting in irregular EBs.

Modest effect of DA in hESC differentiation

Dependent on the differentiation protocol used and time of DA exposure, our results suggest a modest role for DA in increasing the number of dopaminergic neurons derived from hESCs in vitro. Although we quantified a 73% increase in number of TH^+ clusters per coverslip (Fig. 7), we chose to characterize this effect as "modest" because application of dbcAMP alone causes equal or stronger boosting of the number of TH^+ (putative dopaminergic) neurons in hESC culture. Since dbcAMP is already the principal ingredient in the established DA differentiation protocols [21,22], it is important to reiterate that replacement of dbcAMP by DA, or adding DA on top of dbcAMP, has no practical value. Conditioning of the culture media with dbcAMP, or with PA6 stromal cells alone, is a better strategy for production of human DA neurons than the stimulation of DA receptors *per se*. However, this is not to say that stimulation of DA receptors had no effect on proliferation of neurons or acquisition of the dopaminergic neuron type in hESC cultures. On the contrary, DA treatment clearly produced a greater number of DA neurons than DA-free culture media (Fig. 7). This effect was partially due to an overall increase in the number of postmitotic neurons, especially when DA was included in the early stages of the protocol (Fig. 6). Although our present study did not produce a desired improvement in stem cell technology, it revealed several interesting aspects of dopaminergic signaling in hESCs, listed below.

(1) Based on mRNA and protein expression, D2-like DA receptors (D2, D3, and D4) predominate over the D1-like receptors (D1 and D5) during derivation of neurons from hESCs. D1 is the receptor subtype with the lowest representation in this system.
(2) D1/D5 agonist SKF38393 and D2/D3/D4 agonist quinpirole both induce release of calcium ions from the internal stores in H9 hESCs. The same hESC colony responds to both drugs, consistent with the coexpression of D1-like and D2-like DA receptor subtypes in undifferentiated H9 hESCs (Figs. 1 and 2).
(3) To determine whether dopaminergic drugs could improve the yield of DA neurons from hESCs, we tested DA, 2 DA receptor agonists and 2 DA receptor antagonists. Each drug was applied at 2 time points, early and late in the protocol. To our best knowledge, this is the most systematic analysis of the dopaminergic potential for improving the hESC-neurodifferentiation protocol. We did not find any evidence that DA can outperform or improve the already established dbcAMP-based DA differentiation protocol [22]. Yet, DA by itself positively stimulates the proliferation of TH^+ neurons.
(4) Rather than improving the yield of midbrain DA neurons, late treatment with either DA [10 μM], or SKF83566 [0.5 μM] or L741 [0.5 μM] caused a decrease in the expression of midbrain markers (Fig. 9).
(5) D1/D5 antagonist (SKF83566), when applied in the beginning of the hESC neurodifferentiation protocol (Early Treatment), caused morphological changes in EBs (Fig. 4C), a delay in transition from EB to NE (Fig. 4D), and improved the expression of midbrain markers (Fig. $9E_5$–E_7). Expression of D5 mRNA (Fig. $1B_2$) and D5 protein (Fig. 2), physiological response to D1/D5 agonist (Fig. 3) and the surprising effect of D5 antagonist on midbrain markers (Fig. 9), when combined suggest that constitutive activity of D5 receptors [67] in the early stages of the dbcAMP-based protocol (Stages 1–3) affects in vitro neurodifferentiation of H9 hESCs.
(6) In the absence of dbcAMP, DA boosts the proliferation of neurons (Fig. 6), especially TH^+ neurons (Fig. 7).
(7) DA exposure of stem cells differentiating on PA6 mouse stromal cells also resulted in increased expression of TH compared to DA-free PA6-stem cell cocultures.

(8) DA treatment did not affect the physiological (electrical) properties of young neurons, including the transmembrane Na^+ and K^+ currents, or AP firing.
(9) Inclusion of D2-antagonist L741 in the culture media caused a severe reduction in the number of TH^+ clusters (Fig. 7E), consistent with the L741-induced decrease in midbrain markers (Fig. $9E_5$–E_7). This effect was not due to blocking the negative effect of D2 receptor on the cAMP pathway, because in our cultures the increase in cAMP boosts TH expression (Fig. 7C; dbcAMP), see also Refs. [21,22]. Rather, the L741-induced reduction in TH clusters should be attributed to the interactions between D2-like receptors and extracellular signal-regulated kinase (ERK), Nurr1 and Ptx3 and Wnt5a [33,37].

Acknowledgments

This study was supported by Connecticut Stem Cell Initiative/Connecticut Innovations grant 09-SCA-UCHC-13 to S.D.A. Experiments on H9 line were performed in agreement with the WICell Institute, Madison, Wisconsin (agreement no. 10-W0292). The authors are grateful to Jingli Cai for introducing the "Iacovitti Lab" differentiation protocol to us; to the Nada Zecevic laboratory for providing fetal brain tissue samples; to Jessica Lennington for her insights on the role of DA in the neuroproliferation; and to the UConn-Wesleyan University Stem Cell Core for supplying hESCs. Electrophysiological and optical measurements were performed in the Stem Cell Physiology and Chemistry Core, which is supported by Connecticut Innovations grant SCD-01–2009.

Author Disclosure Statement

The authors have no competing financial interests.

References

1. Nieoullon A. (2002). Dopamine and the regulation of cognition and attention. Prog Neurobiol 67:53–83.
2. Goto Y and AA Grace. (2007). The dopamine system and the pathophysiology of schizophrenia: a basic science perspective. Int Rev Neurobiol 78C:41–68.
3. Tsui A and O Isacson. (2011). Functions of the nigrostriatal dopaminergic synapse and the use of neurotransplantation in Parkinson's disease. J Neurol 258:1393–1405.
4. Zecevic N and C Verney. (1995). Development of the catecholamine neurons in human embryos and fetuses, with special emphasis on the innervation of the cerebral cortex. J Comp Neurol 351:509–535.
5. Silani V, D Mariani, FM Donato, C Ghezzi, F Mazzucchelli, M Buscaglia, G Pardi and G Scarlato. (1994). Development of dopaminergic neurons in the human mesencephalon and *in vitro* effects of basic fibroblast growth factor treatment. Exp Neurol 128:59–76.
6. Olson L and A Seiger. (1972). Early prenatal ontogeny of central monoamine neurons in the rat: fluorescence histochemical observations. Z Anat Entwicklungsgesch 137:301–316.
7. Spencer GE, J Klumperman and NI Syed. (1998). Neurotransmitters and neurodevelopment. Role of dopamine in neurite outgrowth, target selection and specific synapse formation. Perspect Dev Neurobiol 5:451–467.
8. O'Keeffe GC, P Tyers, D Aarsland, JW Dalley, RA Barker and MA Caldwell. (2009). Dopamine-induced proliferation of adult neural precursor cells in the mammalian subventricular zone is mediated through EGF. Proc Natl Acad Sci U S A 106:8754–8759.
9. Lennington JB, S Pope, AE Goodheart, L Drozdowicz, SB Daniels, JD Salamone and JC Conover. (2011). Midbrain dopamine neurons associated with reward processing innervate the neurogenic subventricular zone. J Neurosci 31:13078–13087.
10. Bodis J, Z Bognar, G Hartmann, A Torok and IF Csaba. (1992). Measurement of noradrenaline, dopamine and serotonin contents in follicular fluid of human graafian follicles after superovulation treatment. Gynecol Obstet Invest 33:165–167.
11. Zhou J, HF Bradford and GM Stern. (1994). The response of human and rat fetal ventral mesencephalon in culture to the brain-derived neurotrophic factor treatment. Brain Res 656:147–156.
12. Erceg S, S Lainez, M Ronaghi, P Stojkovic, MA Perez-Arago, V Moreno-Manzano, R Moreno-Palanques, R Planells-Cases and M Stojkovic. (2008). Differentiation of human embryonic stem cells to regional specific neural precursors in chemically defined medium conditions. PLoS One 3:e2122.
13. Arenas E. (2010). Towards stem cell replacement therapies for Parkinson's disease. Biochem Biophys Res Commun 396:152–156.
14. Zhang XQ and SC Zhang. (2010). Differentiation of neural precursors and dopaminergic neurons from human embryonic stem cells. Methods Mol Biol 584:355–366.
15. Darsalia V, SJ Allison, C Cusulin, E Monni, D Kuzdas, T Kallur, O Lindvall and Z Kokaia. (2010). Cell number and timing of transplantation determine survival of human neural stem cell grafts in stroke-damaged rat brain. J Cereb Blood Flow Metab 31:235–242.
16. Chung S, JI Moon, A Leung, D Aldrich, S Lukianov, Y Kitayama, S Park, Y Li, VY Bolshakov, T Lamonerie and KS Kim. (2011). ES cell-derived renewable and functional midbrain dopaminergic progenitors. Proc Natl Acad Sci U S A 108:9703–9708.
17. Lindvall O and Z Kokaia. (2010). Stem cells in human neurodegenerative disorders—time for clinical translation? J Clin Invest 120:29–40.
18. Correia AS, SV Anisimov, L Roybon, JY Li and P Brundin. (2007). Fibroblast growth factor-20 increases the yield of midbrain dopaminergic neurons derived from human embryonic stem cells. Front Neuroanat 1: 4.
19. Winner B, DM Vogt-Weisenhorn, CD Lie, I Blumcke and J Winkler. (2009). Cellular repair strategies in Parkinson's disease. Ther Adv Neurol Disord 2:51–60.
20. Zhang TA, AN Placzek and JA Dani. (2010). *In vitro* identification and electrophysiological characterization of dopamine neurons in the ventral tegmental area. Neuropharmacology 59:431–436.
21. Belinsky GS, AR Moore, SM Short, MT Rich and SD Antic. (2011). Physiological properties of neurons derived from human embryonic stem cells using a dibutyryl cyclic AMP-based protocol. Stem Cells Dev 10:1733–1746.
22. Iacovitti L, AE Donaldson, CE Marshall, S Suon and M Yang. (2007). A protocol for the differentiation of human embryonic stem cells into dopaminergic neurons using only chemically defined human additives: studies *in vitro* and *in vivo*. Brain Res 1127:19–25.
23. Wang X, X Li, K Wang, H Zhou, B Xue and L Li. (2004). Forskolin cooperating with growth factor on generation of

dopaminergic neurons from human fetal mesencephalic neural progenitor cells. Neurosci Lett 362:117–121.
24. Stull ND and L Iacovitti. (2001). Sonic hedgehog and FGF8: inadequate signals for the differentiation of a dopamine phenotype in mouse and human neurons in culture. Exp Neurol 169:36–43.
25. Callier S, M Snapyan, S Le Crom, D Prou, JD Vincent and P Vernier. (2003). Evolution and cell biology of dopamine receptors in vertebrates. Biol Cell 95:489–502.
26. Maggio R, G Aloisi, E Silvano, M Rossi and MJ Millan. (2009). Heterodimerization of dopamine receptors: new insights into functional and therapeutic significance. Parkinsonism Relat Disord 15 Suppl 4:S2–7.
27. Beaulieu JM and RR Gainetdinov. (2011). The physiology, signaling, and pharmacology of dopamine receptors. Pharmacol Rev 63:182–217.
28. Moore AR, R Filipovic, Z Mo, MN Rasband, N Zecevic and SD Antic. (2009). Electrical excitability of early neurons in the human cerebral cortex during the second trimester of gestation. Cereb Cortex 19:1795–1805.
29. Zhou WL and SD Antic. (2012). Rapid dopaminergic and GABAergic modulation of calcium and voltage transients in dendrites of prefrontal cortex pyramidal neurons. J Physiol 590:3891–3911.
30. Zecevic N. (2004). Specific characteristic of radial glia in the human fetal telencephalon. Glia 48:27–35.
31. Hersch SM, BJ Ciliax, CA Gutekunst, HD Rees, CJ Heilman, KK Yung, JP Bolam, E Ince, H Yi and AI Levey. (1995). Electron microscopic analysis of D1 and D2 dopamine receptor proteins in the dorsal striatum and their synaptic relationships with motor corticostriatal afferents. J Neurosci 15:5222–5237.
32. Lee SP, CH So, AJ Rashid, G Varghese, R Cheng, AJ Lanca, BF O'Dowd and SR George. (2004). Dopamine D1 and D2 receptor co-activation generates a novel phospholipase C-mediated calcium signal. J Biol Chem 279:35671–35678.
33. Kim SY, KC Choi, MS Chang, MH Kim, YS Na, JE Lee, BK Jin, BH Lee and JH Baik. (2006). The dopamine D2 receptor regulates the development of dopaminergic neurons via extracellular signal-regulated kinase and Nurr1 activation. J Neurosci 26:4567–4576.
34. Tremblay RG, M Sikorska, JK Sandhu, P Lanthier, M Ribecco-Lutkiewicz and M Bani-Yaghoub. (2010). Differentiation of mouse Neuro 2A cells into dopamine neurons. J Neurosci Methods 186:60–67.
35. McIlvain HB, A Baudy, K Sullivan, D Liu, K Pong, M Fennell and J Dunlop. (2006). Pituitary adenylate cyclase-activating peptide (PACAP) induces differentiation in the neuronal F11 cell line through a PKA-dependent pathway. Brain Res 1077:16–23.
36. Kulagowski JJ, HB Broughton, NR Curtis, IM Mawer, MP Ridgill, R Baker, F Emms, SB Freedman, R Marwood, et al. (1996). 3-((4-(4-Chlorophenyl)piperazin-1-yl)-methyl)-1H-pyrrolo-2,3-b-pyridine: an antagonist with high affinity and selectivity for the human dopamine D4 receptor. J Med Chem 39:1941–1942.
37. Collo G, S Zanetti, C Missale and P Spano. (2008). Dopamine D3 receptor-preferring agonists increase dendrite arborization of mesencephalic dopaminergic neurons via extracellular signal-regulated kinase phosphorylation. Eur J Neurosci 28:1231–1240.
38. Adler S, C Pellizzer, M Paparella, T Hartung and S Bremer. (2006). The effects of solvents on embryonic stem cell differentiation. Toxicol In Vitro 20:265–271.
39. Summerhill EM, K Wood and MC Fishman. (1987). Regulation of tyrosine hydroxylase gene expression during differentiation of neuroblastoma cells. Brain Res 388:99–103.
40. Yan Y, D Yang, ED Zarnowska, Z Du, B Werbel, C Valliere, RA Pearce, JA Thomson and SC Zhang. (2005). Directed differentiation of dopaminergic neuronal subtypes from human embryonic stem cells. Stem Cells 23:781–790.
41. Sonntag KC, J Pruszak, T Yoshizaki, J van Arensbergen, R Sanchez-Pernaute and O Isacson. (2007). Enhanced yield of neuroepithelial precursors and midbrain-like dopaminergic neurons from human embryonic stem cells using the bone morphogenic protein antagonist noggin. Stem Cells 25:411–418.
42. Park CH, YK Minn, JY Lee, DH Choi, MY Chang, JW Shim, JY Ko, HC Koh, MJ Kang, et al. (2005). *In vitro* and *in vivo* analyses of human embryonic stem cell-derived dopamine neurons. J Neurochem 92:1265–1276.
43. Perrier AL, V Tabar, T Barberi, ME Rubio, J Bruses, N Topf, NL Harrison and L Studer. (2004). Derivation of midbrain dopamine neurons from human embryonic stem cells. Proc Natl Acad Sci U S A 101:12543–12548.
44. Park S, KS Lee, YJ Lee, HA Shin, HY Cho, KC Wang, YS Kim, HT Lee, KS Chung, EY Kim and J Lim. (2004). Generation of dopaminergic neurons *in vitro* from human embryonic stem cells treated with neurotrophic factors. Neurosci Lett 359:99–103.
45. Schulz TC, SA Noggle, GM Palmarini, DA Weiler, IG Lyons, KA Pensa, AC Meedeniya, BP Davidson, NA Lambert and BG Condie. (2004). Differentiation of human embryonic stem cells to dopaminergic neurons in serum-free suspension culture. Stem Cells 22:1218–1238.
46. Schuldiner M, R Eiges, A Eden, O Yanuka, J Itskovitz-Eldor, RS Goldstein and N Benvenisty. (2001). Induced neuronal differentiation of human embryonic stem cells. Brain Res 913:201–205.
47. Young A, KS Assey, CD Sturkie, FD West, DW Machacek and SL Stice. (2010). Glial cell line-derived neurotrophic factor enhances *in vitro* differentiation of mid-/hindbrain neural progenitor cells to dopaminergic-like neurons. J Neurosci Res 88:3222–3232.
48. Lee MY, JS Heo and HJ Han. (2006). Dopamine regulates cell cycle regulatory proteins via cAMP, Ca(2+)/PKC, MAPKs, and NF-kappaB in mouse embryonic stem cells. J Cell Physiol 208:399–406.
49. Voorn P, A Kalsbeek, B Jorritsma-Byham and HJ Groenewegen. (1988). The pre- and postnatal development of the dopaminergic cell groups in the ventral mesencephalon and the dopaminergic innervation of the striatum of the rat. Neuroscience 25:857–887.
50. Diaz J, S Ridray, V Mignon, N Griffon, JC Schwartz and P Sokoloff. (1997). Selective expression of dopamine D3 receptor mRNA in proliferative zones during embryonic development of the rat brain. J Neurosci 17:4282–4292.
51. Ohtani N, T Goto, C Waeber and PG Bhide. (2003). Dopamine modulates cell cycle in the lateral ganglionic eminence. J Neurosci 23:2840–2850.
52. Van Kampen JM, T Hagg and HA Robertson. (2004). Induction of neurogenesis in the adult rat subventricular zone and neostriatum following dopamine D3 receptor stimulation. Eur J Neurosci 19:2377–2387.
53. Kim Y, WZ Wang, I Comte, E Pastrana, PB Tran, J Brown, RJ Miller, F Doetsch, Z Molnâar and F Szele. (2010). Dopamine stimulation of postnatal murine subventricular zone neurogenesis via the D3 receptor. J Neurochem 114:750–760.

54. Milosevic J, SC Schwarz, M Maisel, M Poppe-Wagner, MT Dieterlen, A Storch and J Schwarz. (2007). Dopamine D2/D3 receptor stimulation fails to promote dopaminergic neurogenesis of murine and human midbrain-derived neural precursor cells *in vitro*. Stem Cells Dev 16:625–635.
55. Van Kampen JM and HA Robertson. (2005). A possible role for dopamine D3 receptor stimulation in the induction of neurogenesis in the adult rat substantia nigra. Neuroscience 136:381–386.
56. Yu P, Z Yang, JE Jones, Z Wang, SA Owens, SC Mueller, RA Felder and PA Jose. (2004). D1 dopamine receptor signaling involves caveolin-2 in HEK-293 cells. Kidney Int 66:2167–2180.
57. Levey AI, SM Hersch, DB Rye, RK Sunahara, HB Niznik, CA Kitt, DL Price, R Maggio, MR Brann and BJ Ciliax. (1993). Localization of D1 and D2 dopamine receptors in brain with subtype-specific antibodies. Proc Natl Acad Sci U S A 90:8861–8865.
58. Fishburn CS, Z Elazar and S Fuchs. (1995). Differential glycosylation and intracellular trafficking for the long and short isoforms of the D2 dopamine receptor. J Biol Chem 270:29819–29824.
59. Schalling M, A Dagerlind, M Goldstein, M Ehrlich, P Greengard and T Hokfelt. (1990). Comparison of gene expression of the dopamine D-2 receptor and DARPP-32 in rat brain, pituitary and adrenal gland. Eur J Pharmacol 188:277–281.
60. Frohna PA, BS Neal-Beliveau and JN Joyce. (1995). Neonatal 6-hydroxydopamine lesions lead to opposing changes in the levels of dopamine receptors and their messenger RNAs. Neuroscience 68:505–518.
61. Qian Y, B Hitzemann, GL Yount, JD White and R Hitzemann. (1993). D1 and D2 dopamine receptor turnover and D2 messenger RNA levels in the neuroleptic-responsive and the neuroleptic nonresponsive lines of mice. J Pharmacol Exp Ther 267:1582–1590.
62. Apati A, K Paszty, Z Erdei, K Szebenyi, L Homolya and B Sarkadi. (2012). Calcium signaling in pluripotent stem cells. Mol Cell Endocrinol 353:57–67.
63. Malmersjo S, I Liste, O Dyachok, A Tengholm, E Arenas and P Uhlen. (2010). Ca2+ and cAMP signaling in human embryonic stem cell-derived dopamine neurons. Stem Cells Dev 19:1355–1364.
64. Todd RD. (1992). Neural development is regulated by classical neurotransmitters: dopamine D2 receptor stimulation enhances neurite outgrowth. Biol Psychiatry 31:794–807.
65. Schmidt U, C Beyer, AB Oestreicher, I Reisert, K Schilling and C Pilgrim. (1996). Activation of dopaminergic D1 receptors promotes morphogenesis of developing striatal neurons. Neuroscience 74:453–460.
66. Swarzenski BC, L Tang, YJ Oh, KL O'Malley and RD Todd. (1994). Morphogenic potentials of D2, D3, and D4 dopamine receptors revealed in transfected neuronal cell lines. Proc Natl Acad Sci U S A 91:649–653.
67. Tiberi M and MG Caron. (1994). High agonist-independent activity is a distinguishing feature of the dopamine D1B receptor subtype. J Biol Chem 269:27925–27931.
68. Zhang X, CT Huang, J Chen, MT Pankratz, J Xi, J Li, Y Yang, TM Lavaute, XJ Li, et al. (2010). Pax6 is a human neuroectoderm cell fate determinant. Cell Stem Cell 7:90–100.
69. Bjorklund A and SB Dunnett. (2007). Dopamine neuron systems in the brain: an update. Trends Neurosci 30:194–202.
70. Maye P, S Becker, E Kasameyer, N Byrd and L Grabel. (2000). Indian hedgehog signaling in extraembryonic endoderm and ectoderm differentiation in ES embryoid bodies. Mech Dev 94:117–132.

Address correspondence to:
Dr. Srdjan D. Antic
Department of Neuroscience
UConn Health Center
263 Farmington Avenue
Farmington, CT 06030-3401

E-mail: antic@neuron.uchc.edu

Received for publication March 30, 2012
Accepted after revision January 3, 2013
Prepublished on Liebert Instant Online January 3, 2013